

Transcriptome wide association study of coronary artery disease identifies novel susceptibility genes

Heribert Schunkert (✉ schunkert@dhm.mhn.de)

Deutsches Herzzentrum München, Technische Universität München, Munich <https://orcid.org/0000-0001-6428-3001>

Ling Li

Deutsches Herzzentrum München <https://orcid.org/0000-0002-3280-9475>

Zhifen Chen

Deutsches Herzzentrum München

Moritz Scheidt

Deutsches Herzzentrum München

Andrea Steiner

Deutsches Herzzentrum München

Ulrich Guldener

German Heart Centre Munich <https://orcid.org/0000-0001-5052-8610>

Simon Koplev

Icahn School of Medicine at Mount Sinai

Angela Ma

Icahn School of Medicine at Mount Sinai

Ke Hao

Mount Sinai School of Medicine

Calvin Pan

University of California Los Angeles <https://orcid.org/0000-0002-0752-833X>

Aldons Lusic

University of California Los Angeles <https://orcid.org/0000-0001-9013-0228>

Shichao Pang

Technical University of Munich

Thorsten Kessler

Technical University Munich <https://orcid.org/0000-0003-3326-1621>

Raili Ermel

Tartu University Hospital <https://orcid.org/0000-0002-2726-2364>

Katyayani Sukhvasi

Department of Cardiac Surgery and The Heart Clinic, Tartu University Hospital <https://orcid.org/0000-0001-5627-0163>

Arno Ruusalepp

Tartu University Hospital

Julien Gagneur

Technical University Munich <https://orcid.org/0000-0002-8924-8365>

Jeanette Erdmann

Universität zu Lübeck <https://orcid.org/0000-0002-4486-6231>

Jason Kovacic

Icahn School of Medicine at Mount Sinai <https://orcid.org/0000-0003-4555-769X>

Johan Bjorkegren

Icahn School of Medicine, Mount Sinai <https://orcid.org/0000-0003-1945-7425>

Article

Keywords: coronary artery disease (CAD), transcriptome-wide association studies (TWAS), novel susceptibility genes

Posted Date: July 27th, 2021

DOI: <https://doi.org/10.21203/rs.3.rs-678054/v1>

License:  This work is licensed under a Creative Commons Attribution 4.0 International License.

[Read Full License](#)

1 Transcriptome wide association study of coronary artery 2 disease identifies novel susceptibility genes

3 Ling Li^{1,2,3†}; Zhifen Chen^{1,3†}; Moritz von Scheidt^{1,3}; Andrea Steiner^{1,3}; Ulrich Güldener^{1,3};
4 Simon Koplev⁴; Angela Ma⁴; Ke Hao⁴; Calvin Pan⁵; Aldons J. Lusis^{5,6,7}; Shichao Pang^{1,3};
5 Thorsten Kessler^{1,7}; Raili Ermel⁸; Katyayani Sukhvasi⁸; Arno Ruusalepp^{8,9}; Julien Gagneur²;
6 Jeanette Erdmann^{10,11}; Jason C. Kovacic^{12,13}; Johan L.M. Björkegren^{4,9,14}; Heribert
7 Schunkert^{1,3}

8 ¹ Department of Cardiology, Deutsches Herzzentrum München, Technische Universität Mün-
9 chen, Germany

10 ² Center for Doctoral Studies in Informatics and its Applications, Department of Informatics,
11 Technische Universität München, Germany

12 ³ Deutsches Zentrum für Herz- und Kreislaufforschung (DZHK), Munich Heart Alliance,
13 Munich, Germany

14 ⁴Department of Genetics & Genomic Sciences, Institute of Genomics and Multiscale Biology,
15 Icahn School of Medicine at Mount Sinai, New York, NY, 10029-6574, USA

16 ⁵Department of Human Genetics, David Geffen School of Medicine, University of California,
17 Los Angeles, California, USA

18 ⁶Departments of Medicine, David Geffen School of Medicine, University of California, Los
19 Angeles, California, USA

20 ⁷ Departments of Microbiology, Immunology and Molecular Genetics, David Geffen School
21 of Medicine, University of California, Los Angeles, California, USA

22 ⁸ Department of Cardiac Surgery and The Heart Clinic, Tartu University Hospital, Tartu,
23 Estonia

24 ⁹ Clinical Gene Networks AB, Stockholm, Sweden

25 ¹⁰ DZHK (German Research Centre for Cardiovascular Research), Partner Site
26 Hamburg/Lübeck/Kiel, Lübeck, Germany.

27 ¹¹ Institute for Cardiogenetics, University of Lübeck, Maria-Geoppert-Str. 1, Lübeck, Germany.

28 ¹² Victor Chang Cardiac Research Institute, Darlinghurst, Australia; and St Vincent's Clinical
29 School, University of New South Wales, Australia

30 ¹³ Cardiovascular Research Institute, Icahn School of Medicine at Mount Sinai, New York, NY,
31 10029-6574, USA

32 ¹⁴ Department of Medicine, Huddinge, Karolinska Institutet, Karolinska Universitetssjukhuset,
33 Stockholm, Sweden

34 † These two authors contributed equally to this work.

35 **Address for correspondence:**

36 Heribert Schunkert, MD

37 German Heart Center Munich, Technical University Munich

38 Lazarettstraße 36, 80636 Munich, Germany

39 Tel.: +49 89 1218 4073 schunkert@dhm.mhn.de

40

41 **Abstract**

42 **Transcriptome-wide association studies (TWAS) explore genetic variants affecting gene**
43 **expression for association with a trait. Here we studied coronary artery disease (CAD)**
44 **using this approach by first determining genotype-regulated expression levels in nine**
45 **CAD relevant tissues by EpiXcan in two genetics-of-gene-expression panels, the**
46 **Stockholm-Tartu Atherosclerosis Reverse Network Engineering Task (STARNET) and**
47 **the Genotype-Tissue Expression (GTEx). Based on these data we next imputed gene**
48 **expression in respective nine tissues from individual level genotype data on 37,997 CAD**
49 **cases and 42,854 controls for a subsequent gene-trait association analysis.**

50 **Transcriptome-wide significant association ($P < 3.85e-6$) was observed for 114 genes,**
51 **which by genetic means were differentially expressed predominately in arterial, liver,**
52 **and fat tissues. Of these, 96 resided within previously identified GWAS risk loci and 18**
53 **were novel (*CAND1, EGFLAM, EZR, FAM114A1, FOCAD, GAS8, HOMER3, KPTN,***
54 ***MGP, NLRC4, RGS19, SDCCAG3, STX4, TSPAN11, TXNRD3, UFL1, WASF1, and***
55 ***WWP2*). Gene set analyses showed that TWAS genes were strongly enriched in CAD-**
56 **related pathways and risk traits. Associations with CAD or related traits were also**
57 **observed for damaging mutations in 67 of these TWAS genes (11 novel) in whole-exome**
58 **sequencing data of UK Biobank. Association studies in human genotype data of UK**
59 **Biobank and expression-trait association statistics of atherosclerosis mouse models**
60 **suggested that newly identified genes predominantly affect lipid metabolism, a classic**
61 **risk factor for CAD. Finally, CRISPR/Cas9-based gene knockdown of *RGS19* and**
62 ***KPTN* in a human hepatocyte cell line resulted in reduced secretion of APOB100 and**
63 **lipids in the cell culture medium. Taken together, our TWAS approach was able to i)**
64 **prioritize genes at known GWAS risk loci and ii) identify novel genes which are**
65 **associated with CAD.**

66 **Introduction**

67 Coronary artery disease (CAD), a leading cause of premature death worldwide, is influenced
68 by interactions of lifestyle, environmental, and genetic risk factors¹. Genome-wide
69 association studies (GWAS) have identified over 200 risk loci for CAD^{2,3}. Most of them are
70 located in non-coding regions which hampers their functional interpretation. Expression
71 quantitative traits loci (eQTLs) to some extent explain the genomic effects of GWAS
72 signals⁴⁻⁶. By leveraging effects of multiple *cis*-eQTL variants on gene expression,
73 transcriptome-wide association studies (TWAS) search primarily for gene-trait associations.
74 The approach builds on predictive models of gene expression derived from reference panels
75 that correlate genotype patterns with transcript levels in tissues which are relevant for the
76 phenotype. Predictive models are then used to associate tissue-specific gene expression based
77 on genotypes with a given trait in individuals of GWAS cohorts⁷. Since TWAS signals reflect
78 gene expression levels, the approach can be used to prioritize candidate genes across disease-
79 relevant tissues. Thereby, TWAS may point to causal genes at risk loci identified by GWAS
80 and thus provide further insights on biological mechanisms^{8,9}. Moreover, TWAS increase the
81 sensitivity to identify susceptibility genes missed by traditional GWAS analyses. Here we
82 performed a TWAS to identify novel susceptibility genes for CAD comprising more than
83 80,000 individuals with genotype data along with validation and exploratory analyses for the
84 associated genes.

85 **Results**

86 **Evaluation of the predictive models from STARNET and GTEx panels**

87 The study design is shown in Fig. 1. We applied predictive models of nine tissues trained by
88 the EpiXcan pipeline⁹ from two genetics-of-gene-expression panels: Stockholm-Tartu
89 Atherosclerosis Reverse Network Engineering Task (STARNET) and Genotype-Tissue

90 Expression (GTEx)^{10,11}. STARNET is a genetics-of-gene-expression study on approximately
91 600 CAD patients undergoing open-heart surgery, during which seven tissues were collected:
92 atherosclerotic aortic wall (AOR), atherosclerotic-lesion-free internal mammary artery
93 (MAM), liver (LIV), blood (BLD), subcutaneous fat (SF), visceral abdominal fat (VAF), and
94 skeletal muscle (SKLM)¹⁰. GTEx is a comprehensive resource for genetics-of-gene-
95 expression across 54 non-diseased tissue sites obtained post-mortem from nearly 1000
96 individuals¹¹. In GTEx we studied six of the above tissues as well as the wall of coronary
97 (COR) and tibial (TIB) arteries, whereas MAM was not available (Methods and
98 Supplementary Tables 1-2). Together, we obtained predictive models from nine CAD-
99 relevant tissues. Genes with cross-validated prediction $R^2 > 0.01$ were kept. STARNET-
100 based models allowed to impute 12,995 unique gene expression signatures in seven tissues,
101 and GTEx 12,964 unique gene expression signatures in eight tissues (Supplementary Table
102 1).

103 We first tested the reproducibility of the STARNET- and GTEx-based predictive
104 models by performing TWAS analyses in ten GWAS studies of CAD covering 17,687 CAD
105 patients and 17,854 controls¹²⁻²¹, which provided individual level data and partially overlap
106 with the CARDIoGRAMplusC4D meta-analysis, followed by replication analyses on
107 genotyping data of UK Biobank (UKB)²², from which we extracted 20,310 CAD patients
108 and 25,000 controls (Supplementary Table 3). As can be seen in Supplementary Results,
109 there were prominent overlaps of transcriptome-wide significant genes having consistent
110 association directions between test and validating sets within STARNET- (binomial test $P =$
111 0.00075) and GTEx-based models (binomial test $P = 0.00079$; Supplementary Fig. 1)
112 respectively. Between the two independent reference panels, TWAS results of six
113 overlapping tissues indicated consistent association directions (average Pearson's coefficient
114 $\rho = 0.72$; $P < 1e-10$; Supplementary Fig. 2), and prominent overlaps of significant gene-tissue

115 pairs (Supplementary Results; Supplementary Fig. 3). Overall, these results suggest the
116 reproducibility of TWAS results of predictive models within and between two independent
117 reference panels.

118 **Genes associated with CAD by TWAS**

119 By combining TWAS results based on two genetics-of-gene-expression reference
120 panels, we identified 114 genes representing 193 gene-tissue pairs with differential
121 expression in CAD cases and controls (Fig. 2; Supplementary Fig. 4; Supplementary Table
122 4). Moreover, 95 of overall 114 gene-tissue association pairs were confirmed using another
123 commonly used fine-mapping tool (COLOC)²³ that calculates the posterior probabilities of
124 shared causal variant in each locus between eQTL and GWAS statistics (Methods;
125 Supplementary Table 5; Supplementary Fig. 5).

126 Forty-six genes displayed genetically-mediated differential expression in AOR, 28 in
127 MAM, 25 in LIV, 23 in VAF, 22 in SKLM, 18 in SF, 16 in BLD, 10 in TIB, and 5 in COR
128 (Fig. 3A), reflecting the importance of respective tissues in CAD pathophysiology. Most
129 genes revealed significant associations in only a single tissue; 38 were significant in more
130 than one, almost all having consistent directions of association between predicted expression
131 levels and CAD across tissues (Fig. 3B).

132 Among the 114 genes, 102 were protein-coding and 12 were long non-coding RNAs
133 (lncRNA) (Supplementary Table 4). STARNET data showed that most lncRNAs were
134 positively co-expressed with a surrounding gene in affected tissues (Supplementary Fig. 8).
135 *LINC00310* was the only exception, which displayed complex co-expression patterns with
136 other genes (Supplementary Fig. 8).

137 Respective genes were found in 63 genomic regions, thus several regions represented
138 multiple genes with significant associations. Six regions had multiple TWAS genes with

139 shared GWAS and eQTL signals in respective tissues, like 1p13.3 and 2p33.2
140 (Supplementary Fig. 6-7; Supplementary Table 5). On the other hand, in 39 regions
141 expression of only a single gene was found to be significantly associated, which makes these
142 genes likely candidates for mediating causal effects, particularly, if these genes reside within
143 GWAS risk loci for CAD (these genes are indicated in Supplementary Table 6).

144 Most TWAS genes (n=96) could be positionally annotated to the 1Mb region around
145 one of the over 200 GWAS loci that are currently known to be genome-wide significantly
146 associated with CAD^{2,3}. Therefore we marked these as known genes (Supplementary Table
147 6). On the other hand, 18 genes resided outside of these regions and were labeled as novel
148 genes (Table 1). Most novel genes were tissue-specific, except *RGS19*, *FAM114A1* and
149 *UFL1* which displayed evidence for differential expression in multiple tissues.

150 **Pathways and diseases enriched by TWAS genes**

151 We carried out two types of gene set enrichment tests to further study the biological
152 relevance of genes giving signals in this TWAS. First, we studied disease-gene sets from the
153 DisGeNET platform which is one of the largest publicly available collections of genes and
154 variants associated with human diseases²⁴. The results showed that genes discovered by
155 TWAS were primarily enriched for CAD, coronary atherosclerosis, and hypercholesterolemia
156 (Supplementary Table 7), adding to the plausibility of our TWAS findings.

157 In line with these results, gene set enrichment analyses using GO²⁵, KEGG²⁶,
158 Reactome²⁷, and WikiPathways²⁸ databases showed that the TWAS genes were highly
159 enriched for pathways involved in cholesterol metabolism and regulation of lipoprotein
160 levels. To a lesser extent, risk genes were enriched in regulation of blood pressure as well as
161 development and morphogenesis of the heart and the aortic valve (Supplementary Table 8).

162 **Damaging mutations in TWAS genes**

163 We next searched in whole-exome sequencing data of 200,643 participants from UKB for
164 rare damaging variants in TWAS genes (minor allele frequency < 0.01, either loss of function
165 mutations or mutations predicted to be adverse by one of five in-silico methods
166 (Supplementary Files). We performed gene-based burden test on major CAD-related
167 cardiometabolic risk traits. We found evidence for nominally significant association with
168 either CAD or its risk traits for 67 TWAS genes (Fig. 4; Supplementary Tables 9-10).
169 Mutations in five genes were directly associated with increased CAD risk: *LPL* (odds ratio
170 [OR] = 1.168; 95% confidence interval [CI] 1.034-1.036; P = 0.016), *NOS3* (OR = 1.143;
171 95% CI 1.109-1.279; P = 0.02), *ADAMTS7* (OR = 1.062; 95% CI 1.011-1.115; P = 0.016),
172 *MTAP* (OR=1.507; 95%CI 1.061-2.086; P = 0.017), and *HLA-C* (OR = 1.112; 95%CI 1.002-
173 1.239; P = 0.044); and two were associated reduced CAD risk: *TWIST1* (OR = 0.726; 95% CI
174 0.523-0.985; P = 0.038), *SARS* (OR = 0.831; 95% CI 0.706-0.974; P = 0.022). Damaging
175 *LPL* mutations were evidently associated with lipid traits, including levels of LDL (low
176 density lipoproteins) (beta = 0.043; P = 9.6e-4), HDL (high density lipoproteins) (beta = -
177 0.106; P = 4.54e-68), APOA (Apolipoprotein A) (beta = -0.062; P = 6.25e-47), APOB
178 (Apolipoprotein B) (beta = 0.025; P = 1.38e-12), and TG (Triglycerides) (beta = 0.241; P =
179 1.47e-68).

180 Damaging mutations in 11 novel TWAS genes were associated with CAD risk factors
181 (Table 2). Some of these gene-trait associations have been reported before. Damaging
182 mutations in *MGP*, which regulates vascular calcification, adipogenesis and is serum marker
183 of visceral adiposity²⁹⁻³¹, were associated with increased levels of LDL, TC (total
184 cholesterol) and APOB. *NLRC4* was reportedly associated with atherosclerosis by regulating
185 inflammation reaction^{32,33}, and its damaging mutations were associated with levels of CRP
186 (C-reactive protein – a marker of inflammation).

187 **Novel genes associate with risk factors in human and mouse data**

188 We next associated common variants in the regions of ± 1 Mb around the 18 novel TWAS
189 genes to study their associations with a series of lipid traits including LDL, HDL, APOA,
190 APOB, LPA, TC, and TG in UKB (Supplementary Files). Bonferroni-corrected significance
191 $P < 4.0 \times 10^{-4}$ ($0.05/18$ novel genes * 7 lipid traits) was observed for numerous respective lead
192 variants, of which *RGS19*, *SDCCAG3*, *HOMER3*, and *WWP2* reached genome-wide
193 significant association ($P < 5 \times 10^{-8}$) with multiple lipid traits (Fig. 5A; Supplementary Table 11).

194 Next, we extracted expression-trait association statistics of TWAS genes from the
195 Hybrid Mouse Diversity Panel (HMDP)³⁴. Based on the expression data from mouse aorta
196 and liver tissues, 48 TWAS genes were significantly associated with aortic lesion area and 14
197 further cardiovascular traits (nominal significance $P < 0.05$; Supplementary Table 12).
198 Expression levels of seven novel genes, i.e. *Rgs19*, *Kptn*, *Ezr*, *Stx4a*, *Cand1*, *Focad* and
199 *Wasf1*, were associated with aortic lesion area (Fig. 5B), a commonly used measure for
200 atherosclerotic plaque formation in mice. Additionally, we found the novel genes were
201 associated with at least one lipid trait in the mouse model (Fig. 5B).

202 **Knockdown of *RGS19* and *KPTN* reduced lipid secretion by human liver cells**

203 Both human genotype-trait association statistics in UKB and mouse expression-trait
204 association statistics in the HMDP indicated that several novel genes identified by TWAS
205 influence lipid metabolism. To validate these findings, we chose two of the novel genes, i.e.
206 *KPTN* and *RGS19*, which have not been studied in much detail so far and have particularly
207 not at all been investigated in the context of atherosclerosis or CAD. Hepatocytes are
208 critically involved in lipid metabolism. In line, in a screening of different atherosclerosis-
209 relevant cell lines (e.g., hepatocytes, smooth muscle, endothelium, fibroblast, and
210 adipocytes), *KPTN* had the highest expression level in the huh7 hepatocyte cell line

211 (Supplementary Fig. 9A, B). To study the influence of *KPTN* and *RGS19* on lipid
212 metabolism, we next generated gene knockout (KO) huh7 cell lines for by a dual CRISPR
213 strategy (Methods; Supplementary Table 13), which substantially reduced expression of the
214 respective genes (Supplementary Fig. 9C, D). We measured secretion levels of TG,
215 cholesterol and APOB in gene-targeted versus control cells. Notably, under normal
216 circumstances, human hepatocytes synthesize cholesterol, assemble TG and APOB100, and
217 secrete these particles in form of very low-density lipoprotein (VLDL)³⁵. Compared to
218 control huh7 cells, we found reduced APOB and cholesterol levels in culture medium of
219 *KPTN*-KO cells (Fig. 6C, D). In culture medium of *RGS19*-KO cells we also detected
220 reduced levels of APOB100, cholesterol, and TG (Fig. 6B, C, D, E), in line with strong
221 associations of this gene with an array of lipid traits in both human genotyping and mouse
222 expression data sets (Figure 5).

223 **Discussion**

224 In a stepwise approach, we first generated and filtered models predicting genetically
225 modulated gene expression in nine tissues that contribute to CAD risk. Next, we applied
226 these models to individual-level genotype data on more than 80,000 CAD cases and controls.
227 We identified 114 genes with differential expression by genetic means in CAD patients.
228 Many signals were highly plausible as they resided within loci displaying genome-wide
229 significant association with CAD by traditional GWAS. Moreover, the genes identified by
230 this TWAS were markedly enriched in established pathways for the disease, and 67 revealed
231 in whole-exome sequence data of UKB that damaging mutations have significant impact on
232 CAD risk or its underlying traits. Importantly, we also identified 18 genes without prior
233 evidence for their involvement in CAD by GWAS, many of which were found to be
234 associated with lipid metabolism in human and mouse data.

235 Only a minority of genes residing within published CAD GWAS loci have been
236 validated experimentally for their underlying causal role in atherosclerosis. Our data
237 corroborate a recent exploration of known GWAS loci for genotype-related expression levels
238 (Hao et al., personal communication, manuscript attached) and provide a substantial step
239 towards prioritization of genes at respective GWAS loci^{2,3}. In this respect, 46 genes identified
240 by this TWAS are known for effects in pathophysiological pathways related to CAD,
241 including lipid metabolism, inflammation, angiogenesis, transcriptional regulation, cell
242 proliferation, NO signaling, and high blood pressure, to name a few (Supplementary Table 6),
243 giving credibility to the association findings. On the other hand, a limitation of the TWAS
244 approach is that at 20 loci two or more genes show signals such that other methods will be
245 needed to pinpoint the precise genetic mechanisms leading to CAD. Indeed, in another study
246 we recently applied summary-based Mendelian Randomization, MetaXcan, to integrate tissue
247 and cell-specific data from STARNET and GTEx with CAD GWAS datasets, and obtained at
248 14 of these 20 loci indicative data allowing prioritization of a gene (Hao et al., personal
249 communication, manuscript attached).

250 Most novel TWAS genes revealed association with lipid traits in both genotype data
251 of human and expression-trait statistics of our atherosclerosis mouse model. For example,
252 expression profiles of *KPTN* and *RGS19*, both novel genes displaying significant TWAS
253 results for CAD in human liver tissue, also showed significant association with various lipid
254 traits as well as aortic lesion area in our atherosclerosis mouse model. Moreover, both gene
255 loci harbor SNPs which are genome-wide significantly associated with LDL-C, HDL-C, TC,
256 and TG in human genotype data. Finally, the Common Metabolic Disease Knowledge Portal
257 revealed that damaging rare variants of *KPTN* are associated with reduced levels of LDL
258 (beta = -11.9; P = 0.00042) and TC (beta = -11.9; P = 0.0014)³⁶, which is directionally
259 plausible given the TWAS results. Based on these observations, we functionally validated the

260 roles of these two novel genes by studying lipid levels in human liver cells, i.e. the tissue that
261 displayed evidence for differential expression by TWAS. Indeed, we observed that knockout
262 of these genes lowered secretion of APOB and cholesterol into culture medium. *KPTN*,
263 kaptin (actin binding protein), a member of the *KPTN*, *ITFG2*, *C12orf66* and *SZT2*
264 (KICSTOR) protein complex, is a lysosome-associated negative regulator of the mechanistic
265 target of rapamycin complex 1 (mTORC1) signaling³⁷. It is required in amino acid or glucose
266 deprivation to inhibit cell growth by suppressing mTORC1 signaling in liver, muscle, and
267 neurons. mTORC1 has multifaceted roles in regulating lipid metabolism, including the
268 promotion of lipid synthesis, and storage and inhibition of lipid release and consumption,
269 suggesting that the validated role of *KPTN* in hepatic lipid secretion might be partially
270 mediated by the mTORC1 pathway. *RGS19* belongs to the *RGS* (regulators of G-protein
271 signaling) family, who are regulators for G protein-coupled receptors (GPCRs)³⁸. *RGS19*
272 inhibits GPCR signal transduction by increasing the GTPase activity of G protein alpha
273 subunits, thereby transforming them into an inactive GDP-bound form^{39,40}. The targeting
274 GPCR of *RGS19* has not been observed before, and how *RGS19* regulates lipid metabolism
275 remains unclear.

276 Interestingly, our TWAS uncovered eight novel gene-CAD associations in fat tissue,
277 including *MGP* and *WASF1* in SF, and *CAND1*, *FAM114A1*, *FOCAD*, *RGS19*, *TSPAN11* and
278 *TXNRD3* in VAF, representing half of the novel genes. Damaging mutations in five genes
279 were associated with many cardiometabolic risk factors for CAD, including those in *WASF1*
280 with BMI, *MGP* with LDL, TC and APOB, *TXNRD3* with LPA, *FAM114A1* with diabetes,
281 *FOCAD* with hypertension, i.e. conditions shown by Mendelian randomization to be causal
282 for CAD⁴¹. Given the many CAD patients that are overweight or obese, it will be of great
283 interest to identify how these genes modify cardiometabolic traits leading to cardiovascular
284 disorders. In this respect our TWAS could provide a list of candidate genes and related

285 targetable cardiometabolic traits. In addition, it is of surprise to unveil 22 genes linking
286 SKLM to CAD risk, and eight were unique to this tissue, including *HOMER3*, *SDCCAG3*,
287 *MTAP*, *NME9*, *PSMA4*, *SLC2A12*, *UNC119B* and *VAMP5*, , the first two being novel.
288 *SDCCAG3* or *ENTRI* encodes endosome associated trafficking regulator 1 and involves in
289 recycling of *GLUT1* (glucose transporter type 1), supplying the major energy source for
290 muscle contraction. SKLM-based metabolism may have a protective role in CAD as
291 suggested by the many cardioprotective effects of sports^{42,43}. Gene targets enhancing SKLM
292 function in this respect might be effective in CAD prevention, a field relatively unexplored
293 thus far. Here, for the first time, quantitative traits regulated genes in SKLM were associated
294 with CAD by TWAS, providing novel evidence for genes that could modulate CAD risk by
295 their functions in SKLM.

296 There are certain limitations in our study. Since TWAS are strongly dependent on the
297 reference panel linking genetic signatures with gene expression, it had to be expected that
298 STARNET- and GTEx-based predictive models display differences in gene-CAD
299 associations. STARNET-based TWAS identified 86 genes, whereas GTEx-based TWAS
300 identified 68 genes. Yet, 34 genes were shared between the two analyses, and effect sizes for
301 the shared genes were highly concordant ($\rho = 0.97$). An average of 62% overlapping genes
302 was observed in the matched tissues of two reference-based models, and the resulting size of
303 expression-CAD associations was linearly consistent with an average $\rho = 0.72$. The relatively
304 small differences may be due to different sample sizes used for training predictive models⁹,
305 different disease states (subjects with and without CAD), intravital or *post mortem* sample
306 collection, leading to differences in gene expression in our reference panels^{10,11}. Given a fair
307 consistency between the two data sources, we combined results derived from both panels to
308 increase the power for capturing risk genes. Second, although TWAS facilitates candidate
309 risk gene prioritization, co-regulation or co-expression *in cis* at a given locus limits the

310 precise determination of the culprit gene⁸. Indeed, at 12 loci we observed signals for three or
311 more TWAS genes. For instance, in LIV tissue TWAS identified five genes at 1p13.3,
312 *ATXN7L2*, *CELSR2*, *PSMA5*, *PSRC1*, *SARS* and *SORT1* which were co-regulated by same
313 risk variant set, confusing the causal gene prioritization. While *CELSR2*, *PSRC1* and *SORT1*
314 were previously shown to act on lipid metabolism⁴⁴, we found that damaging mutations in
315 *ATXN7L2* and *SARS* were also associated with CAD or its risk traits, the former with serum
316 levels of HDL and APOA, and the later with CAD and diabetes. In addition, all lncRNA
317 genes identified by our study displayed co-expression with their neighboring coding genes,
318 which makes it difficult to determine their casual effects. Nevertheless, in combining TWAS
319 data with other genetic analyses, e.g., looking at effects of damaging mutations, genetic
320 association with other phenotypes and expression-traits association statistics, we aimed to
321 improve risk gene prioritization, and to provide deeper insights of possible disease-causing
322 mechanisms. For instance, *LPL* is well-known for its protective role against CAD by
323 lowering lipids^{45,46}, and our analyses showed that damaging *LPL* mutations were associated
324 with increased risk of CAD and higher lipid levels. Finally, as with all statistical methods,
325 there are certain limitations and assumptions associated with TWAS. Further evolution and
326 improvement of these methods, as well as functional validation experiments, will assuredly
327 improve the accuracy of these studies.

328 In summary, our TWAS study based on two genotype-expression reference panels
329 identified 114 gene-CAD associations, of which 18 were novel. The extended analyses with
330 multiple datasets supported the reliability of the CAD TWAS signals in prioritizing candidate
331 risk genes and identifying novel associations in a tissue-specific manner. Functional
332 validation of two novel genes, *RGS19* and *KPTN*, lend support to our TWAS findings. Our
333 study created a set of gene-centered and tissue-annotated associations for CAD, providing
334 insightful guidance for further biological investigation and therapeutic development.

335

336 **References**

- 337 1. Malakar, A. K. *et al.* A review on coronary artery disease, its risk factors, and
338 therapeutics. *J. Cell. Physiol.* **234**, 16812–16823 (2019).
- 339 2. Erdmann, J., Kessler, T., Munoz Venegas, L. & Schunkert, H. A decade of genome-
340 wide association studies for coronary artery disease: The challenges ahead.
341 *Cardiovascular Research* vol. 114 1241–1257 (2018).
- 342 3. Koyama, S. *et al.* Population-specific and trans-ancestry genome-wide analyses
343 identify distinct and shared genetic risk loci for coronary artery disease. *Nat. Genet.*
344 **52**, 1169–1177 (2020).
- 345 4. Foroughi Asl, H. *et al.* Expression Quantitative Trait Loci Acting Across Multiple
346 Tissues Are Enriched in Inherited Risk for Coronary Artery Disease. *Circ. Cardiovasc.*
347 *Genet.* **8**, 305–315 (2015).
- 348 5. Wild, P. S. *et al.* A Genome-Wide Association Study Identifies *LIPA* as a
349 Susceptibility Gene for Coronary Artery Disease. *Circ. Cardiovasc. Genet.* **4**, 403–412
350 (2011).
- 351 6. Vilne, B. & Schunkert, H. Integrating Genes Affecting Coronary Artery Disease in
352 Functional Networks by Multi-OMICs Approach. *Frontiers in Cardiovascular*
353 *Medicine* vol. 5 89 (2018).
- 354 7. Gamazon, E. R. *et al.* A gene-based association method for mapping traits using
355 reference transcriptome data. *Nat. Genet.* **47**, 1091–1098 (2015).
- 356 8. Wainberg, M. *et al.* Opportunities and challenges for transcriptome-wide association
357 studies. *Nat. Genet.* **51**, 592–599 (2019).
- 358 9. Zhang, W. *et al.* Integrative transcriptome imputation reveals tissue-specific and
359 shared biological mechanisms mediating susceptibility to complex traits. *Nat.*
360 *Commun.* **10**, 1–13 (2019).

- 361 10. Franzén, O. *et al.* Cardiometabolic risk loci share downstream cis- and trans-gene
362 regulation across tissues and diseases. *Science (80-.)*. **353**, 827–830 (2016).
- 363 11. Lonsdale, J. *et al.* The Genotype-Tissue Expression (GTEx) project. *Nature Genetics*
364 vol. 45 580–585 (2013).
- 365 12. Samani, N. J. *et al.* Genomewide Association Analysis of Coronary Artery Disease. *N.*
366 *Engl. J. Med.* **357**, 443–453 (2007).
- 367 13. Erdmann, J. *et al.* New susceptibility locus for coronary artery disease on chromosome
368 3q22.3. *Nat. Genet.* **41**, 280–282 (2009).
- 369 14. Erdmann, J. *et al.* Genome-wide association study identifies a new locus for coronary
370 artery disease on chromosome 10p11.23. *Eur. Heart J.* **32**, 158–168 (2011).
- 371 15. Nikpay, M. *et al.* A comprehensive 1000 Genomes-based genome-wide association
372 meta-analysis of coronary artery disease. *Nat. Genet.* **47**, 1121–1130 (2015).
- 373 16. Stitzel, N. O. *et al.* Inactivating mutations in NPC1L1 and protection from coronary
374 heart disease. *N. Engl. J. Med.* **371**, 2072–2082 (2014).
- 375 17. Nelson, C. P. *et al.* Association analyses based on false discovery rate implicate new
376 loci for coronary artery disease. *Nat. Genet.* **49**, 1385–1391 (2017).
- 377 18. Li, L., Pang, S., Zeng, L., Güldener, U. & Schunkert, H. Genetically determined
378 intelligence and coronary artery disease risk. *Clin. Res. Cardiol.* (2020)
379 doi:10.1007/s00392-020-01721-x.
- 380 19. Burton, P. R. *et al.* Genome-wide association study of 14,000 cases of seven common
381 diseases and 3,000 shared controls. *Nature* **447**, 661–678 (2007).
- 382 20. Winkelmann, B. R. *et al.* Rationale and design of the LURIC study - A resource for
383 functional genomics, pharmacogenomics and long-term prognosis of cardiovascular
384 disease. *Pharmacogenomics* **2**, (2001).
- 385 21. Anderson, C. D. *et al.* Genome-wide association of early-onset myocardial infarction

- 386 with single nucleotide polymorphisms and copy number variants. *Nat. Genet.* **478**,
387 103–109 (2015).
- 388 22. Bycroft, C. *et al.* The UK Biobank resource with deep phenotyping and genomic data.
389 *Nature* **562**, 203–209 (2018).
- 390 23. Giambartolomei, C. *et al.* Bayesian Test for Colocalisation between Pairs of Genetic
391 Association Studies Using Summary Statistics. *PLoS Genet.* **10**, (2014).
- 392 24. Piñero, J. *et al.* The DisGeNET knowledge platform for disease genomics: 2019
393 update. *Nucleic Acids Res.* **48**, D845–D855 (2020).
- 394 25. Harris, M. A. *et al.* The Gene Oncology (GO) database and informatics resource.
395 *Nucleic Acids Res.* **32**, D258–D261 (2004).
- 396 26. Kanehisa, M. & Goto, S. KEGG: Kyoto Encyclopedia of Genes and Genomes. *Nucleic*
397 *Acids Research* vol. 28 27–30 (2000).
- 398 27. Croft, D. *et al.* Reactome: A database of reactions, pathways and biological processes.
399 *Nucleic Acids Res.* **39**, D691–D697 (2011).
- 400 28. Slenter, D. N. *et al.* WikiPathways: A multifaceted pathway database bridging
401 metabolomics to other omics research. *Nucleic Acids Res.* **46**, D661–D667 (2018).
- 402 29. Bjørklund, G. *et al.* The Role of Matrix Gla Protein (MGP) in Vascular Calcification.
403 *Curr. Med. Chem.* **27**, 1647–1660 (2019).
- 404 30. Okla, M. *et al.* Ellagic acid modulates lipid accumulation in primary human adipocytes
405 and human hepatoma Huh7 cells via discrete mechanisms. *J. Nutr. Biochem.* **26**, 82–90
406 (2015).
- 407 31. Li, C. *et al.* Matrix Gla protein regulates adipogenesis and is serum marker of visceral
408 adiposity. *Adipocyte* **9**, 68–76 (2020).
- 409 32. Borborema, M. E. de A., Crovella, S., Oliveira, D. & de Azevêdo Silva, J.
410 Inflammasome activation by NLRP1 and NLRC4 in patients with coronary stenosis.

- 411 *Immunobiology* **225**, 151940 (2020).
- 412 33. Alehashemi, S. & Goldbach-Mansky, R. Human Autoinflammatory Diseases Mediated
413 by NLRP3-, Pyrin-, NLRP1-, and NLRC4-Inflammasome Dysregulation Updates on
414 Diagnosis, Treatment, and the Respective Roles of IL-1 and IL-18. *Frontiers in*
415 *Immunology* vol. 11 1840 (2020).
- 416 34. Lusis, A. J. *et al.* The hybrid mouse diversity panel: A resource for systems genetics
417 analyses of metabolic and cardiovascular traits. *Journal of Lipid Research* vol. 57
418 925–942 (2016).
- 419 35. Tiwari, S. & Siddiqi, S. A. Intracellular trafficking and secretion of VLDL.
420 *Arteriosclerosis, Thrombosis, and Vascular Biology* vol. 32 1079–1086 (2012).
- 421 36. Flannick, J. *et al.* Exome sequencing of 20,791 cases of type 2 diabetes and
422 24,440 controls. *Nature* **570**, 71–76 (2019).
- 423 37. Wolfson, R. L. *et al.* KICSTOR recruits GATOR1 to the lysosome and is necessary for
424 nutrients to regulate mTORC1. *Nature* **543**, 438–442 (2017).
- 425 38. Oishi, Y. *et al.* SREBP1 Contributes to Resolution of Pro-inflammatory TLR4
426 Signaling by Reprogramming Fatty Acid Metabolism. *Cell Metab.* **25**, 412–427
427 (2017).
- 428 39. Tso, P. H., Yung, L. Y., Wang, Y. & Wong, Y. H. RGS19 stimulates cell proliferation
429 by deregulating cell cycle control and enhancing Akt signaling. *Cancer Lett.* **309**, 199–
430 208 (2011).
- 431 40. Sangphech, N., Osborne, B. A. & Palaga, T. Notch signaling regulates the
432 phosphorylation of Akt and survival of lipopolysaccharide-activated macrophages via
433 regulator of G protein signaling 19 (RGS19). *Immunobiology* **219**, 653–660 (2014).
- 434 41. Jansen, H., Samani, N. J. & Schunkert, H. Mendelian randomization studies in
435 coronary artery disease. *European Heart Journal* vol. 35 1917–1924 (2014).

- 436 42. McGough, I. J. *et al.* Identification of molecular heterogeneity in SNX27-
437 retromermediated endosome-to-plasma-membrane recycling. *J. Cell Sci.* **127**, 4940–
438 4953 (2014).
- 439 43. Sixt, S. *et al.* Long- but not short-term multifactorial intervention with focus on
440 exercise training improves coronary endothelial dysfunction in diabetes mellitus type 2
441 and coronary artery disease. *Eur. Heart J.* **31**, 112–119 (2010).
- 442 44. Arvind, P., Nair, J., Jambunathan, S., Kakkar, V. V. & Shanker, J. CELSR2-PSRC1-
443 SORT1 gene expression and association with coronary artery disease and plasma lipid
444 levels in an Asian Indian cohort. *J. Cardiol.* **64**, 339–346 (2014).
- 445 45. Coding Variation in ANGPTL4, LPL, and SVEP1 and the Risk of Coronary Disease .
446 *N. Engl. J. Med.* **374**, 1134–1144 (2016).
- 447 46. Tsutsumi, K. Lipoprotein Lipase and Atherosclerosis. *Curr. Vasc. Pharmacol.* **1**, 11–
448 17 (2003).
- 449
450

451 **Tables**452 **Table 1 18 TWAS genes residing outside of published GWAS loci.**

Gene	Tissue	Gene type	Cytoband	Z score	SE	P value	From ^a
NLRC4	LIV	protein_coding	2p22.3	-3.383	0.044	3.04E-06	STARNET
TXNRD3	VAF	protein_coding	3q21.3	2.566	0.059	1.36E-06	STARNET
FAM114A1	VAF	protein_coding	4p14	4.026	0.050	3.44E-09	GTEEx
FAM114A1	BLD	protein_coding	4p14	4.845	0.037	1.80E-06	GTEEx
EGFLAM	COR	protein_coding	5p13.2	5.596	0.047	7.70E-10	GTEEx
UFL1	MAM	protein_coding	6q16.1	-5.246	0.038	1.62E-06	STARNET
UFL1	BLD	protein_coding	6q16.1	-4.687	0.038	8.70E-05	STARNET
UFL1	BLD	protein_coding	6q16.1	-4.955	0.042	3.96E-07	GTEEx
WASF1	SF	protein_coding	6q21	4.320	0.059	1.91E-06	STARNET
EZR	LIV	protein_coding	6q25.3	-3.187	0.025	3.53E-06	STARNET
FOCAD	VAF	protein_coding	9p21.3	8.348	0.068	1.44E-12	GTEEx
SDCCAG3	SKLM	protein_coding	9q34.3	-3.015	0.061	1.74E-06	STARNET
TSPAN11	VAF	protein_coding	12p11.21	2.285	0.065	1.79E-07	STARNET
MGP	SF	protein_coding	12p12.3	-3.412	0.040	5.67E-07	GTEEx
CAND1	VAF	protein_coding	12q14.3	-2.355	0.030	1.19E-07	GTEEx
STX4	COR	protein_coding	16p11.2	3.347	0.056	2.59E-06	GTEEx
WWP2	AOR	protein_coding	16q22.1	4.491	0.029	5.67E-06	STARNET
WWP2	AOR	protein_coding	16q22.1	6.570	0.031	1.19E-07	GTEEx
GAS8	LIV	protein_coding	16q24.3	0.189	0.041	8.32E-07	GTEEx
HOMER3	SKLM	protein_coding	19p13.11	4.647	0.030	3.52E-08	GTEEx
KPTN	LIV	protein_coding	19q13.32	-3.076	0.076	2.17E-06	STARNET
RGS19	LIV	protein_coding	20q13.33	-4.913	0.028	1.52E-06	GTEEx
RGS19	VAF	protein_coding	20q13.33	-4.868	0.059	4.51E-06	STARNET
RGS19	VAF	protein_coding	20q13.33	-4.545	0.030	4.63E-07	GTEEx
RGS19	SKLM	protein_coding	20q13.33	-5.026	0.024	1.42E-06	STARNET
RGS19	SKLM	protein_coding	20q13.33	-5.298	0.018	9.29E-07	GTEEx

453 ^a Association statistics from either STARNET- or GTEEx-based models.

454

455

456 **Table 2 Associations of damaging mutations in novel genes with risk traits of CAD.**

Binary trait	Gene	Case		Control		OR[95%CI]	P value
		Non-carrier	Carrier	Non-carrier	Carrier		
Diabetes	FAM114A1	10668	116	187555	1457	1.4[1.15-1.69]	9.19E-04
Diabetes	UFL1	10634	150	187023	1989	1.33[1.11-1.57]	1.47E-03
Hypertension	FOCAD	73542	4605	102379	6129	1.05[1.01-1.09]	2.60E-02
Hypertension	EGFLAM	73754	4393	102147	6361	0.96[0.92-1]	2.82E-02
Hypertension	EZR	77495	652	107491	1017	0.89[0.8-0.98]	2.05E-02

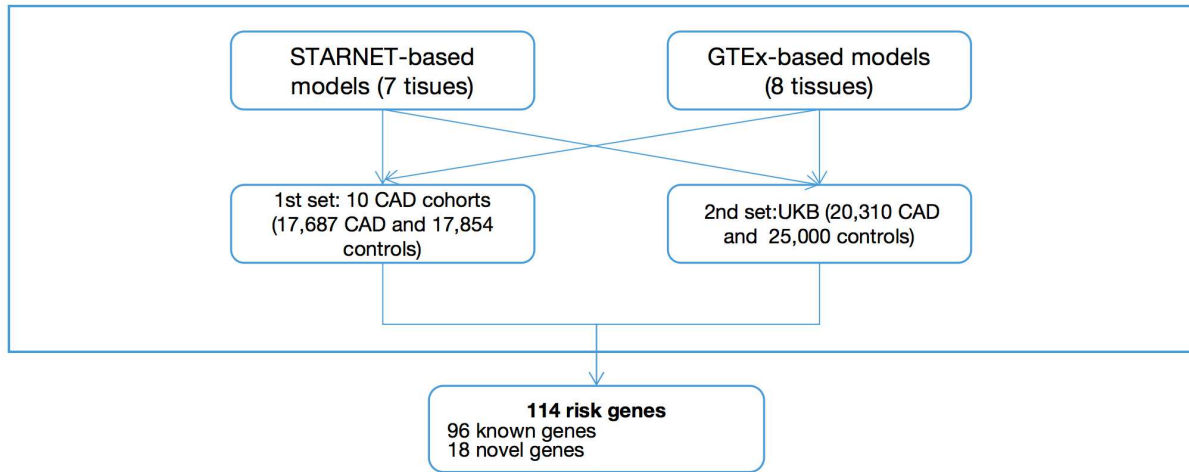
Quantitative trait	Gene	Carrier		Non-carrier		Beta[95%CI]	P value
		No. carrier	Median(range)	No. non-carrier	Median (range)		
APOB (g/L)	HOMER3	2633	1(0.41-1.91)	187891	1.02(0.4-2)	-0.02[-0.03--0.01]	4.02E-03
APOB (g/L)	MGP	158	1.05(0.51-1.96)	190366	1.02(0.4-2)	0.08[0.04-0.13]	2.60E-04
TC (mmol/L)	HOMER3	2651	5.57(2.33-10.06)	188814	5.66(1.64-15.46)	-0.08[-0.14--0.03]	2.95E-03
TC (mmol/L)	MGP	158	5.76(3.19-10.29)	191307	5.66(1.64-15.46)	0.34[0.13-0.56]	1.66E-03
LDL (mmol/L)	HOMER3	2649	3.45(1.05-6.97)	188511	3.52(0.28-9.8)	-0.06[-0.11--0.02]	2.34E-03
LDL (mmol/L)	MGP	158	3.59(1.81-7.05)	191002	3.52(0.28-9.8)	0.29[0.13-0.45]	4.82E-04
LPA (nmol/L)	TXNRD3	3162	21.94(3.8-188.89)	150645	20.98(3.8-189)	2.5[0.29-4.71]	2.63E-02
BMI (kg/m2)	KPTN	2084	26.87(14.94-56.05)	197753	26.7(12.12-68.95)	-0.3[-0.57--0.04]	2.65E-02
BMI (kg/m2)	WASF1	806	26.92(17.71-53.02)	199031	26.7(12.12-68.95)	0.47[0.04-0.91]	3.38E-02
CRP (mg/L)	NLRC4	2470	1.25(0.11-52.86)	188577	1.31(0.08-79.49)	-0.22[-0.44--0.01]	4.30E-02
CRP (mg/L)	UFL1	2057	1.3(0.1-43.74)	188990	1.31(0.08-79.49)	-0.37[-0.6--0.13]	2.36E-03
Neutrophil (10 ⁹ cells/L)	MGP	164	3.51(0.61-8.21)	194782	4.07(0-25.95)	-0.33[-0.59--0.07]	1.40E-02

457

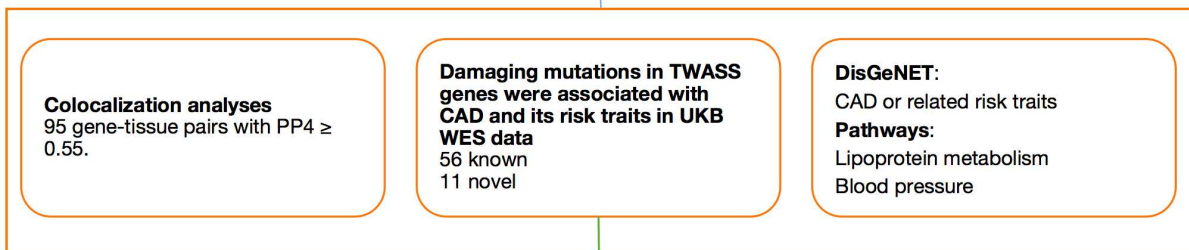
458

459

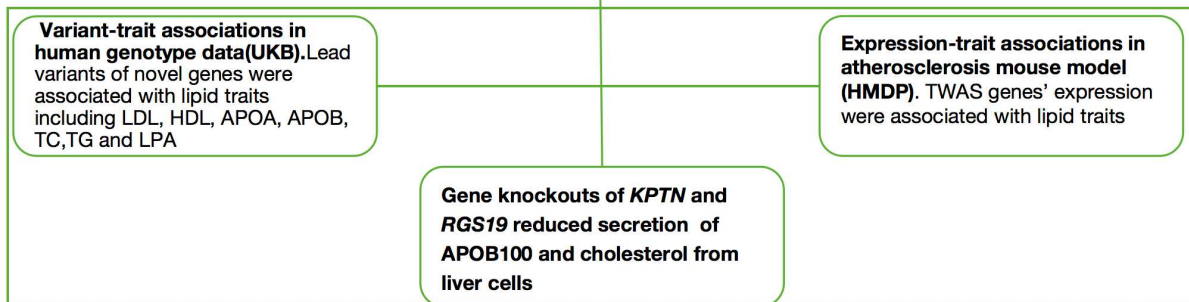
Step1 result reproducibility inside and between two reference-based models



Step2 plausibility, biological function and pathogenicity of TWAS genes (mainly known genes)



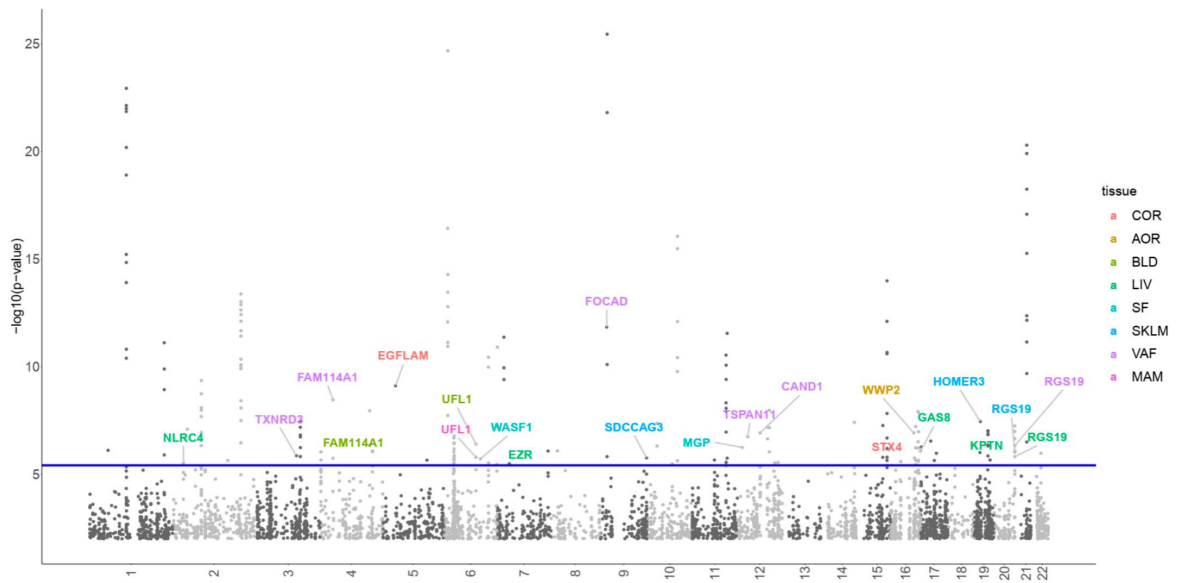
Step3 susceptibility of novel genes



461

462 **Fig. 1 The study design.**

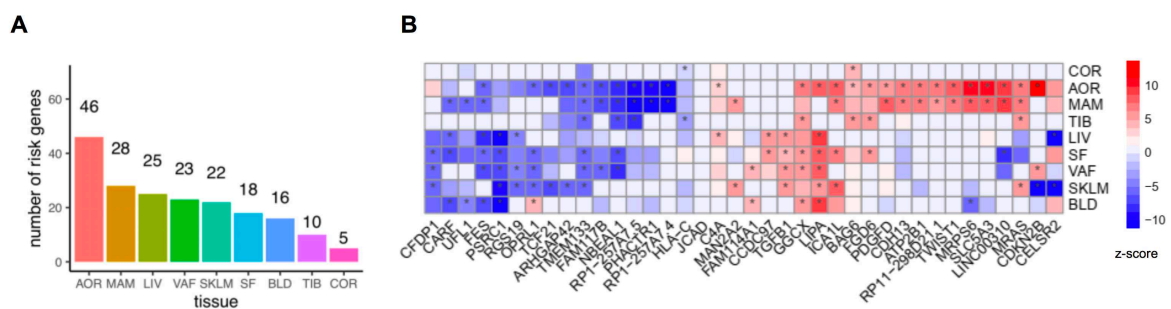
463



464

465 **Fig. 2** Manhattan plot of the transcriptome wide association study (TWAS). The results
 466 from STARNET- and GTEx-based TWASs were integrated by lowest P values. The blue line
 467 marks $P = 3.85 \times 10^{-6}$. Each point corresponds to an association test between gene-tissue pair. 18
 468 novel TWAS genes were highlighted. Supplementary Fig. 4 identifies all genes identified by
 469 their genetically-modulated association signals.

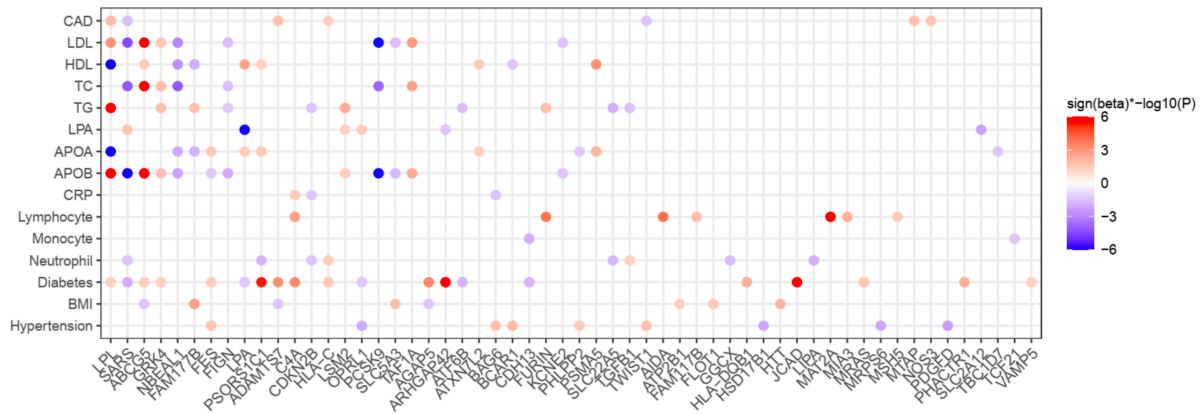
470



471

472 **Fig. 3** Tissue distribution of 114 CAD TWAS genes. (A) Number of significant genes
 473 across tissues. (B) Heatmap plot of 38 TWAS genes identified in more than one tissues. The
 474 color codes indicate direction of effects. Cells marked with * represent significant gene-tissue
 475 pairs ($P < 3.85 \times 10^{-6}$).

476



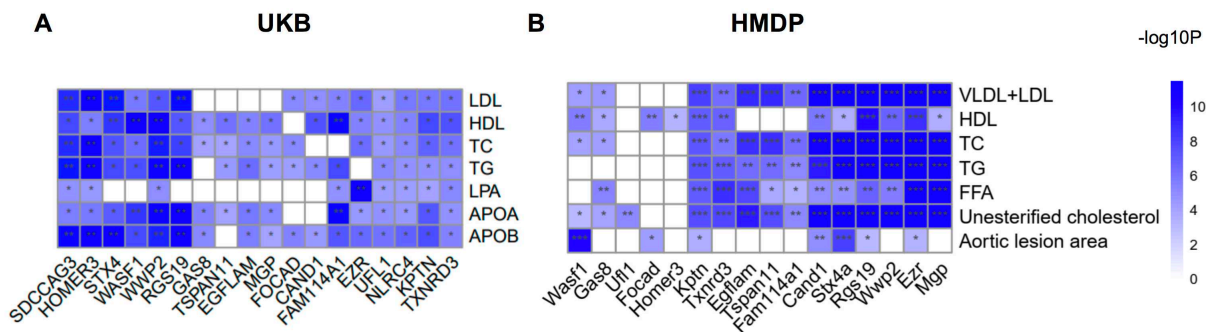
477

478 **Fig. 4 Effects of damaging mutations of TWAS genes on CAD and its risk traits.**

479 Sign(beta)*-log10(p) displayed for associations that reached a P < 0.05. When the

480 Sign(beta)*-log10(P) > 6, they were trimmed to 6

481



482

483 **Fig. 5 Novel risk genes were associated with lipid traits.** (A) Data from UKB indicate that

484 lead variants inside the boundary of risk genes were associated with lipid traits with

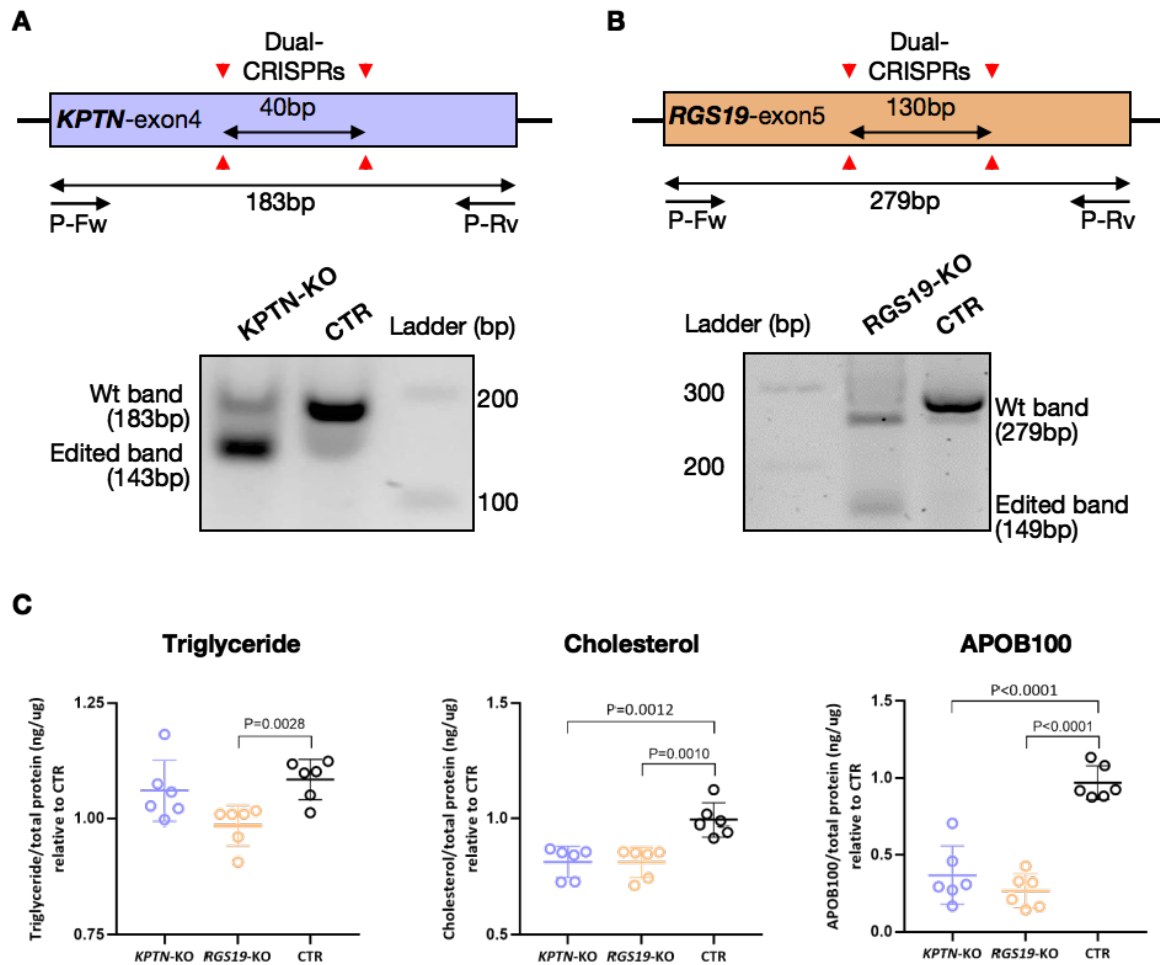
485 Bonferroni-corrected significance levels (*, P < 4.0e-4), or by genome-wide significance (**,

486 P < 5e-8). (B) Expression levels of novel genes were likewise associated with lipid traits and

487 aortic lesion area in an atherosclerosis mouse model from the Hybrid Mouse Diversity Panel

488 (HMDP). *, P < 0.05; **, P < 0.01; ***, P < 0.001.

489



490

491 **Fig. 6 Targeting of *KPTN* and *RGS19* reduced Lipids and APOB secretion of human**

492 **liver cells.** (A) Two sgRNAs were used to target the exon4 of *KPTN* (shared exon among

493 isoforms) in a Cas9-expressing huh7 liver cell line. The dual CRISPR strategy created a 40bp

494 frame shift deletion in the gene and proud reduction of *KPTN* at both mRNA and protein

495 levels (Supplementary Figure 9C, 9D). The primers (P-Fw and P-Rv) used for analyzing the

496 CRISPR editing as indicated. (B) The same strategy was used for *RGS19* targeting, which

497 resulted in a 130bp frame shift deletion in the gene, and reduction of mRNA and protein

498 (Supplementary Figure 9C, 9D). (C) Reduced triglyceride and cholesterol levels in knockout

499 (KO) cell lines were detected by colorimetric method and APOB100 secretion was measured

500 by human APOB100 Elisa (n=6). Triglyceride, cholesterol and APOB100 levels were

501 normalized to total protein and compared between the KO and control (CTR) cell lines.

502

503 **Methods**

504 **Predictive models of nine tissues based on two reference panels**

505 We adopted the existing predictive models trained using EpiXcan pipeline by Zhang et al.¹,
506 including models of atherosclerotic aortic wall (AOR), atherosclerotic-lesion-free internal
507 mammary artery (MAM), liver (LIV), blood (BLD), subcutaneous fat (SF), visceral abdominal
508 fat (VAF) and skeletal muscle (SKLM) based on the genetics-of-gene-expression panel
509 STARNET (The Stockholm-Tartu Atherosclerosis Reverse Network Engineering Task)², and
510 of AOR, LIV, BLD, SF, VAF and SKLM based on GTEx (Genotype-Tissue Expression)³.

511 Arterial wall coronary (COR) and tibial artery (TIB), datasets were only available in
512 the GTEx panel. So, we established predictive models for these two tissues using EpiXcan
513 pipeline as has been done for other models before¹. In brief, we firstly filtered the genotype
514 and expression data of COR and TIB from GTEx v7. Variants with call rate < 0.95, minor
515 allele frequency (MAF) < 0.01, and Hardy Weinberg equilibrium (HWE) < 1e-6 were removed.
516 For expression, we used quality-controlled data and performed sample-level quantile
517 normalization, and gene-level inverse quantile normalization using preprocess codes of
518 PredicDB pipeline. Samples were restrained to the European ethnicity. We then calculated SNP
519 priors by using hierarchical Bayesian model (qtlBHM)⁴ that jointly analyzed epigenome
520 annotations of aorta derived from Roadmap Epigenomics Mapping Consortium (REMC)⁵, and
521 eQTL statistics. The SNP priors (Supplementary Table 2), genotype data and expression data
522 were jointly applied to 10-fold cross-validated weighted elastic-net to train predicting models
523 by deploying EpiXcan pipeline¹.

524 Both STARNET- and GTEx-based models were filtered by cross-validated prediction
525 $R^2 > 0.01$. The summary statistics of sample sizes used for training models and the transcript
526 numbers of genes covered by each predicting models are shown in Supplementary Table 1.

527 **Genotype cohorts**

528 For the discovery cohort, individual level genotyping data were collected from ten genome-
529 wide associations studies (GWAS) of coronary artery disease (CAD), a subset of
530 CARDIoGRAMplusC4D, including the German Myocardial Infarction Family Studies
531 (GerMIFS) I-VII⁶⁻¹², Wellcome Trust Case Control Consortium (WTCCC)¹³, LURIC study¹⁴
532 and Myocardial Infarction Genetics Consortium (MIGen)¹⁵. We used a part of individual-level
533 data from UK Biobank (UKB) as the replication cohort¹⁶, by extracting 20,310 CAD cases
534 according to hospital episodes or death registries as reported, and randomly selected 25,000
535 non-CAD UKB participants as controls. The detailed information about selection criteria of
536 case and control were described at elsewhere¹². In total, genotyping data of 37,997 cases and
537 42,854 controls were included in our transcriptome-wide association studies (TWAS) of CAD
538 (Supplementary Table 3). The preprocessing steps of genotyping data are as previously¹².

539 **Transcriptome wide association analysis**

540 We applied predictive models to the eleven genotype cohorts to impute individual-level
541 expression profiles of nine tissues, and performed transcriptome-wide association analysis
542 between imputed expression and CAD. To test the reproducibility of TWAS results, we
543 performed two types of validating tests: within and between two reference-based models.
544 Firstly, we used ten GWAS cohorts as testing set and UKB as the validating set to test
545 reproducibility within STARNET- and GTEx-based models respectively. Secondly, we
546 compared the consistency of results between STARNET- and GTEx-based models of the six
547 overlapping tissues using all genotype data.

548 **Co-expression network for lncRNA**

549 We used RNA-seq data of STARNET² to calculate expression correlations between long non-
550 coding RNA (lncRNA) genes and protein coding genes in seven tissues. Co-expression pairs
551 with absolute Pearson correlation coefficient larger than 0.4 were considered to be significant.
552 The co-expression network was displayed by cytoscape¹⁷.

553 **Colocalization of the eQTL and GWAS signals**

554 Colocalization analysis was performed using COLOC, a Bayesian statistical methodology that
555 takes GWAS and eQTL data as inputs, and tests the posterior probabilities (PP4) of shared
556 casual variant for each locus¹⁸. The summary statistics of GWAS meta-analysis were obtained
557 from CARDIoGRAMplusC4D Consortium¹¹, and the eQTL data of nine tissues from
558 STARNET² and GTEx³ respectively.

559 **Annotation of novel risk genes**

560 Over 200 CAD loci were identified by GWAS^{19,20}. We used MAGMA²¹ to annotate the 114
561 TWAS genes and observed that 96 genes resided within $\pm 1\text{Mb}$ around known CAD loci
562 whereas 18 genes (novel loci) were located outside known GWAS risk loci, i.e. they were
563 novel genes (Supplementary Table 6).

564 **Gene set enrichment analyses**

565 Pathway enrichment analysis was carried out using ClueGO (v2.5.2)²², a plugin of cytoscape¹⁷,
566 based on collated gene sets from public databases including GO²³, KEGG²⁴, Reactome²⁵, and
567 WikiPathways²⁶. Gene sets with false discovery rate (FDR) by right-sided hypergeometric test
568 less than 0.05 were considered to be significant.

569 Furthermore, we also studied the diseases or traits associated with risk genes by
570 performing disease enrichment analysis based on DisGeNET²⁷, the largest publicly available
571 datasets of genes and variants association of human diseases. FDR < 0.05 was used for
572 thresholding.

573 **Rare damaging variants association analysis**

574 To investigate association of damaging variants in TWAS genes with CAD, we used whole
575 exome sequencing (WES) data of 200,632 participants from UKB²⁸. The WES data was
576 processed following the Functional Equivalence (FE) protocol. We performed quality control
577 on the WES data by filtering variants with calling rate < 0.9, variants with HWE < 1e-6. For
578 the relevant traits, besides CAD, we considered several risk factors of the disease, including
579 body mass index (BMI), diabetes, hypertension, levels of low density lipoproteins (LDL), high
580 density lipoproteins (HDL), apolipoprotein A (APOA), apolipoprotein B (APOB),
581 Lipoprotein(a) (LPA), total cholesterol (TC) and triglycerides (TG)), as well as inflammation
582 related factors (C-reactive protein (CRP), lymphocyte count (Lymphocyte), monocyte count
583 (Monocyte) and neutrophil count (Neutrophil).

584 We defined damaging mutations as i) rare mutations with MAF < 0.01; ii) annotated
585 into following one of the 3 classes: loss-of-function (LoF) (stop-gained, splice site disrupting,
586 or frameshift variants), variants annotated as the pathogenic in ClinVar²⁹, or missense variants
587 predicted to be damaging by one of five computer prediction algorithms (LRT score,
588 MutationTaster, PolyPhen-2 HumDiv, PolyPhen-2 HumVar, and SIFT). The Ensembl Variant
589 Effect Predictor (VEP)³⁰ and its plugin loftee³¹, and annotation databases dbNSFP 4.1a³² and
590 ClinVar (GRCh38)²⁹ were used for annotating damaging mutations.

591 For each analysis, samples were classified into carriers or noncarriers of the gene's
592 damaging mutations. For binary traits, we used Fisher's exact test to check if there was

593 incidences difference of mutation carrying between case and controls. For the quantitative traits,
594 we used linear regression model with adjustments of sex, first five principal components, and
595 lipid medication status to investigate the associations between mutation carrying status and
596 traits. We used nominal significance threshold ($P < 0.05$), given that coding variants are rather
597 rare, and the case-control sample sizes were not balanced which might increase false negative
598 rate. We used nominal significance threshold $P < 0.05$, because, at one hand, the case-control
599 size was not balanced which might increase false negative rate, at the other hand, it's an
600 exploratory trial to investigate the potential biological relevance of TWAS genes.

601 **Association of variants resided in novel genes with lipid traits**

602 For 18 novel risk genes, we performed association analysis for variants located in novel gene
603 loci (± 1 Mbase) with lipid traits using genotyping data of UKB. The lipid traits include levels
604 of LDL, HDL, APOA, APOB, LPA, TC and TG. The variants were filtered by $MAF > 0.01$,
605 and imputation info score > 0.4 . The association test was performed using PLINK2³³ with
606 adjustment of sex, first five principal components, and lipid medication status. The lead
607 variants residing in gene loci with P value less than $4.0e-4$ ($0.05/18$ risk genes * 7 lipid traits)
608 were considered to be significant (Supplementary Table 11).

609 **The Hybrid Mouse Diversity Panel (HMDP)**

610 The Hybrid Mouse Diversity Panel (HMDP) is a set of 105 well-characterized inbred mouse
611 strains on a 50% C57BL/6J genetic background³⁴. To specifically study atherosclerosis in the
612 HMDP, transgene implementation of human APOE-Leiden and cholesteryl ester transfer
613 protein was performed, promoting distinct atherosclerotic lesion formation³⁵. A Western diet
614 containing 1% cholesterol was fed for 16 weeks. Subsequently, gene expression was quantified
615 in aorta and liver of these mice and lesion size was assessed in the proximal aorta using oil red

616 O staining. Other 14 related traits were measured too, including liver fibrosed area, body
617 weight, total cholesterol, VLDL (very low-density lipoprotein) + LDL, HDL, TGs, unesterified
618 cholesterol, free fatty acid, IL-1b, IL-6, TNFa, MCP-1, and M-CSF. From HMDP, we extracted
619 significant association pairs between TWAS genes and 15 risk traits by applying significance
620 $P < 0.05$.

621 **Experimental validation of *KPTN* and *RGS19* in human cells**

622 To knock down *KPTN* and *RGS19*, two sgRNAs targeting shared exons of all transcription
623 isoforms were delivered by lentivirus into a Cas9-expression huh7, a human hepatoma cell line.
624 Exon 4 of *KPTN* and exon 5 of *RGS19* were targeted by a dual CRISPR strategy to create a
625 40bp and 130bp frame shift deletion, respectively. SgRNAs were carried by Lenti-Guide-Puro
626 vector (addgene, #52963) and infected cells were treated with 10ug/ml puromycin treatment
627 for 3 days to eliminate the negative cell. Positive targeted cells were expanded in culture and
628 passaged for assays. Cells for measurement of secretive triglycerides, cholesterol and
629 APOB100 were cultured for 16 hours in serum-free medium. Medium triglycerides and
630 cholesterol were enriched for five times by vacuum centrifuge and measured with colorimetric
631 kits, triglyceride (cobas) and CHOL2 (cobas), respectively. The amount of medium APOB100
632 was measured with an ELISA kit (MABTECH).

633 **Methods References**

- 634 1. Zhang, W. *et al.* Integrative transcriptome imputation reveals tissue-specific and
635 shared biological mechanisms mediating susceptibility to complex traits. *Nat.*
636 *Commun.* **10**, 1–13 (2019).
- 637 2. Franzén, O. *et al.* Cardiometabolic risk loci share downstream cis- and trans-gene
638 regulation across tissues and diseases. *Science (80-.).* **353**, 827–830 (2016).
- 639 3. Aguet, F. *et al.* Genetic effects on gene expression across human tissues. *Nature* **550**,

- 640 204–213 (2017).
- 641 4. Li, Y. I. *et al.* RNA splicing is a primary link between genetic variation and disease.
642 *Science (80-.).* **352**, 600–604 (2016).
- 643 5. Bernstein, B. E. *et al.* The NIH roadmap epigenomics mapping consortium. *Nature*
644 *Biotechnology* vol. 28 1045–1048 (2010).
- 645 6. Samani, N. J. *et al.* Genomewide association analysis of coronary artery disease. *N.*
646 *Engl. J. Med.* **357**, 443–453 (2007).
- 647 7. Erdmann, J. *et al.* New susceptibility locus for coronary artery disease on chromosome
648 3q22.3. *Nat. Genet.* **41**, 280–282 (2009).
- 649 8. Erdmann, J. *et al.* Genome-wide association study identifies a new locus for coronary
650 artery disease on chromosome 10p11.23. *Eur. Heart J.* **32**, 158–168 (2011).
- 651 9. Nikpay, M. *et al.* A comprehensive 1000 Genomes-based genome-wide association
652 meta-analysis of coronary artery disease. *Nat. Genet.* **47**, 1121–1130 (2015).
- 653 10. Stitzel, N. O. *et al.* Inactivating mutations in NPC1L1 and protection from coronary
654 heart disease. *N. Engl. J. Med.* **371**, 2072–2082 (2014).
- 655 11. Nelson, C. P. *et al.* Association analyses based on false discovery rate implicate new
656 loci for coronary artery disease. *Nat. Genet.* **49**, 1385–1391 (2017).
- 657 12. Li, L., Pang, S., Zeng, L., Güldener, U. & Schunkert, H. Genetically determined
658 intelligence and coronary artery disease risk. *Clin. Res. Cardiol.* 1–9 (2020)
659 doi:10.1007/s00392-020-01721-x.
- 660 13. Burton, P. R. *et al.* Genome-wide association study of 14,000 cases of seven common
661 diseases and 3,000 shared controls. *Nature* **447**, 661–678 (2007).
- 662 14. Winkelmann, B. R. *et al.* Rationale and design of the LURIC study - A resource for
663 functional genomics, pharmacogenomics and long-term prognosis of cardiovascular
664 disease. *Pharmacogenomics* **2**, (2001).

- 665 15. Anderson, C. D. *et al.* Genome-wide association of early-onset myocardial infarction
666 with single nucleotide polymorphisms and copy number variants. *Nat. Genet.* **478**,
667 103–109 (2015).
- 668 16. Bycroft, C. *et al.* The UK Biobank resource with deep phenotyping and genomic data.
669 *Nature* **562**, 203–209 (2018).
- 670 17. Kohl, M., Wiese, S. & Warscheid, B. Cytoscape: software for visualization and
671 analysis of biological networks. *Methods Mol. Biol.* **696**, 291–303 (2011).
- 672 18. Giambartolomei, C. *et al.* Bayesian Test for Colocalisation between Pairs of Genetic
673 Association Studies Using Summary Statistics. *PLoS Genet.* **10**, (2014).
- 674 19. Erdmann, J., Kessler, T., Munoz Venegas, L. & Schunkert, H. A decade of genome-
675 wide association studies for coronary artery disease: The challenges ahead.
676 *Cardiovascular Research* vol. 114 1241–1257 (2018).
- 677 20. Koyama, S. *et al.* Population-specific and trans-ancestry genome-wide analyses
678 identify distinct and shared genetic risk loci for coronary artery disease. *Nat. Genet.*
679 **52**, 1169–1177 (2020).
- 680 21. De Leeuw, C. A., Mooij, J. M., Heskes, T. & Posthuma, D. MAGMA: Generalized
681 Gene-Set Analysis of GWAS Data. *PLoS Comput Biol* **11**, 1004219 (2015).
- 682 22. Bindea, G. *et al.* ClueGO: A Cytoscape plug-in to decipher functionally grouped gene
683 ontology and pathway annotation networks. *Bioinformatics* **25**, 1091–1093 (2009).
- 684 23. Harris, M. A. *et al.* The Gene Oncology (GO) database and informatics resource.
685 *Nucleic Acids Res.* **32**, D258–D261 (2004).
- 686 24. Kanehisa, M. & Goto, S. KEGG: Kyoto Encyclopedia of Genes and Genomes. *Nucleic*
687 *Acids Research* vol. 28 27–30 (2000).
- 688 25. Croft, D. *et al.* Reactome: A database of reactions, pathways and biological processes.
689 *Nucleic Acids Res.* **39**, D691–D697 (2011).

- 690 26. Slenter, D. N. *et al.* WikiPathways: A multifaceted pathway database bridging
691 metabolomics to other omics research. *Nucleic Acids Res.* **46**, D661–D667 (2018).
- 692 27. Piñero, J. *et al.* The DisGeNET knowledge platform for disease genomics: 2019
693 update. *Nucleic Acids Res.* **48**, D845–D855 (2020).
- 694 28. Van Hout, C. V. *et al.* Exome sequencing and characterization of 49,960 individuals in
695 the UK Biobank. *Nature* **586**, 749–756 (2020).
- 696 29. Landrum, M. J. *et al.* ClinVar: improvements to accessing data. *Nucleic Acids Res.* **48**,
697 835–844 (2019).
- 698 30. McLaren, W. *et al.* The Ensembl Variant Effect Predictor. *Genome Biol.* **17**, (2016).
- 699 31. Karczewski, K. J. *et al.* The mutational constraint spectrum quantified from variation
700 in 141,456 humans. *Nature* **581**, 434–443 (2020).
- 701 32. Dong, C. *et al.* Comparison and integration of deleteriousness prediction methods for
702 nonsynonymous SNVs in whole exome sequencing studies. *Hum. Mol. Genet.* **24**,
703 2125–2137 (2015).
- 704 33. Chang, C. C. *et al.* Second-generation PLINK: rising to the challenge of larger and
705 richer datasets. *Gigascience* **4**, 7 (2015).
- 706 34. Lusk, A. J. *et al.* The hybrid mouse diversity panel: A resource for systems genetics
707 analyses of metabolic and cardiovascular traits. *Journal of Lipid Research* vol. 57
708 925–942 (2016).
- 709 35. Bennett, B. J. *et al.* Genetic Architecture of Atherosclerosis in Mice: A Systems
710 Genetics Analysis of Common Inbred Strains. *PLoS Genet.* **11**, 1005711 (2015).
- 711
- 712

713 **Author Contributions**

714 H.S., L.L., Z.C., designed the study and wrote the manuscript. L.L. ran analyses. Z.C. and
715 A.S. performed experiments. M.V.S, U.G., S.C.P., S.K., C.P. A.J.L., T.K., A.R.,J.A., J.G.,
716 K.H., J.C.K. and J.M.B. provided research data, technical support and gave conceptual
717 advice.

718 **Competing Interest Declaration**

719 The authors declare that there is no known competing financial interests or personal
720 relationships that could have appeared to influence the work reported in this paper.

721 **Source of Funding**

722 The work was funded by the German Federal Ministry of Education and Research (BMBF)
723 within the framework of ERA-NET on Cardiovascular Disease (Druggable-MI-genes:
724 01KL1802), within the scheme of target validation (BlockCAD: 16GW0198K), and within
725 the framework of the e:Med research and funding concept (AbCD-Net: 01ZX1706C). As a
726 Co-applicant of the British Heart Foundation (BHF)/German Centre of Cardiovascular
727 Research (DZHK)-collaboration (DZHK-BHF: 81X2600522) and the Leducq Foundation for
728 Cardiovascular Research (PlaqOmics: 18CVD02), we gratefully acknowledge their funding.
729 Additional support has been received from the German Research Foundation (DFG) as part
730 of the Sonderforschungsbereich SFB 1123 (B02) and the Sonderforschungsbereich SFB TRR
731 267 (B05). Further, we kindly acknowledge the support of the Bavarian State Ministry of
732 Health and Care who funded this work with DigiMed Bayern (grant No: DMB-1805-0001)
733 within its Masterplan “Bayern Digital II” and of the German Federal Ministry of Economics
734 and Energy in its scheme of ModulMax (grant No: ZF4590201BA8).

735 **Tools and Data**

736 EpiXcan pipeline: <https://bitbucket.org/roussoslab/epixcan/src/master/>, and predictive
737 models based on STARNET and GTEx databases: <http://predictdb.org/>

738 [PrediXcan pipeline: https://github.com/hakyim/PrediXcan.](https://github.com/hakyim/PrediXcan)

739 [qlBHM: https://github.com/rajanil/qlBHM](https://github.com/rajanil/qlBHM)

740 STARNET database: [https://www.ncbi.nlm.nih.gov/projects/gap/cgi-](https://www.ncbi.nlm.nih.gov/projects/gap/cgi-bin/study.cgi?study_id=phs001203.v1.p1)

741 [bin/study.cgi?study_id=phs001203.v1.p1.](https://www.ncbi.nlm.nih.gov/projects/gap/cgi-bin/study.cgi?study_id=phs001203.v1.p1) Project ID: 13585.

742 [GTEEx database: https://www.ncbi.nlm.nih.gov/projects/gap/cgi-](https://www.ncbi.nlm.nih.gov/projects/gap/cgi-bin/study.cgi?study_id=phs000424.v8.p2)

743 [bin/study.cgi?study_id=phs000424.v8.p2.](https://www.ncbi.nlm.nih.gov/projects/gap/cgi-bin/study.cgi?study_id=phs000424.v8.p2) Project ID: 20848.

744 UK Biobank: [https://www.ukbiobank.ac.uk/.](https://www.ukbiobank.ac.uk/) Project ID: 25214

745 MAGMA: <https://ctg.cncr.nl/software/magma>

746 R package for colocalization analysis, coloc: [https://cran.r-](https://cran.r-project.org/web/packages/coloc/vignettes/vignette.html)

747 [project.org/web/packages/coloc/vignettes/vignette.html](https://cran.r-project.org/web/packages/coloc/vignettes/vignette.html)

748 DisGeNET: <https://www.disgenet.org/>

749 CARDIoGRAMplusC4D Consortium: <http://www.cardiogramplusc4d.org/>

750

751

752 **Extended data**

753 **Supplementary Results**

754 We tested the reproducibility of the STARNET- and GTEx-based predictive models
755 by performing TWAS analyses in ten GWAS studies of CAD covering 17,687 CAD patients
756 and 17,854 controls¹²⁻²¹, which provided individual level data and partially overlap with the
757 CARDIoGRAMplusC4D meta-analysis, followed by replication analyses on genotyping data
758 of UK Biobank (UKB)²², from which we extracted 20,310 CAD patients and 25,000 controls
759 (Supplementary Table 3). From STARNET-based models, we identified 66 gene-tissue
760 association pairs reaching Bonferroni-corrected significance ($P < 3.85e-6$) in the ten
761 CARDIoGRAMplusC4D cohorts. Of these, 19 also reached Bonferroni-corrected
762 significance in the UKB data, which was significantly more than expected by chance
763 (binomial test $P = 0.00075$), and 50 of 66 gene-tissue association pairs had directionally
764 consistent effects (binomial test $P = 3.33e-5$). We also found strong correlation of the effect
765 sizes ($\rho = 0.74$; $P = 1.3e-12$; Supplementary Fig. 1A) indicating good overall reproducibility
766 of the STARNET-based models.

767 From the GTEx-based models, 47 gene-tissue pairs reached Bonferroni-corrected
768 significance ($P < 3.85e-6$) in the ten CARDIoGRAMplusC4D cohorts, whereof 14 were
769 significant also in UKB (binominal test $P = 0.0079$). Like the STARNET-based models, 39
770 of 44 significant gene-tissue association pairs had consistent direction of effects with a
771 Pearson's coefficient of 0.75 ($P = 1.2e-9$; Supplementary Fig. 1B). The slightly lower
772 numbers of significant gene-tissue association pairs found in the GTEx models may be
773 explained in that predicting models were based on: i) smaller numbers of genotype-
774 expression pairs, ii) unlike STARNET, GTEx consist of apparently healthy tissues and iii)
775 STARNET is a specific collection of CAD patients.

776 Next, we tested consistency of TWAS results between two reference-based models by
777 comparing the results of a meta-analysis on all 11 genotyping data sets. We observed an
778 average of 62% overlapping genes (Supplementary Table 1) and significant correlations of
779 effect sizes (average Pearson's coefficient $\rho = 0.72$; $P < 1e-10$; Supplementary Fig. 2). In the
780 STARNET-based models, we identified 82 genes representing 129 gene-tissue pairs across
781 seven tissues ($P < 3.85e-6$). In the GTEx models, we identified 66 genes representing 106
782 gene-tissue pairs across eight tissues ($P < 3.85e-6$). A total of 42 gene-tissue pairs were
783 significant in both the STARNET- and GTEx-based models (Supplementary Fig. 3A). The
784 overlapping genes were linearly consistent in both effect size (Pearson's coefficient $\rho = 0.99$;
785 $P < 2.2e-16$) and $-\log_{10}P$ (Pearson's coefficient $\rho = 0.82$; $P < 4e-11$) (Supplementary Fig. 3B).
786 Overall, these results suggest, on the one hand, reasonable consistence between the two
787 independent panels and, on the other hand, evidence for capturing complementary expression
788 quantitative signals.
789

790 **Supplementary Tables**

791 Supplementary Table 1. Statistics of nine tissues' predictive models.

792 Supplementary Table 2. SNP priors of COR and TIB tissues.

793 Supplementary Table 3. 11 Genotype cohorts.

794 Supplementary Table 4. 114 TWAS genes list.

795 Supplementary Table 5. 53 TWAS genes have strong evidence of colocalized signals
796 between GWAS and eQTL ($PP4 > 0.55$).

797 Supplementary Table 6. 96 known and 18 novel genes annotated by GWAS risk loci of CAD.

798 Supplementary Table 7. TWAS genes are enriched to CAD or related risk traits based on
799 DisGeNET.

800 Supplementary Table 8. Pathways enriched by TWAS genes.

801 Supplementary Table 9. Association of TWAS genes' damaging mutation with CAD and its
802 binary risk traits.

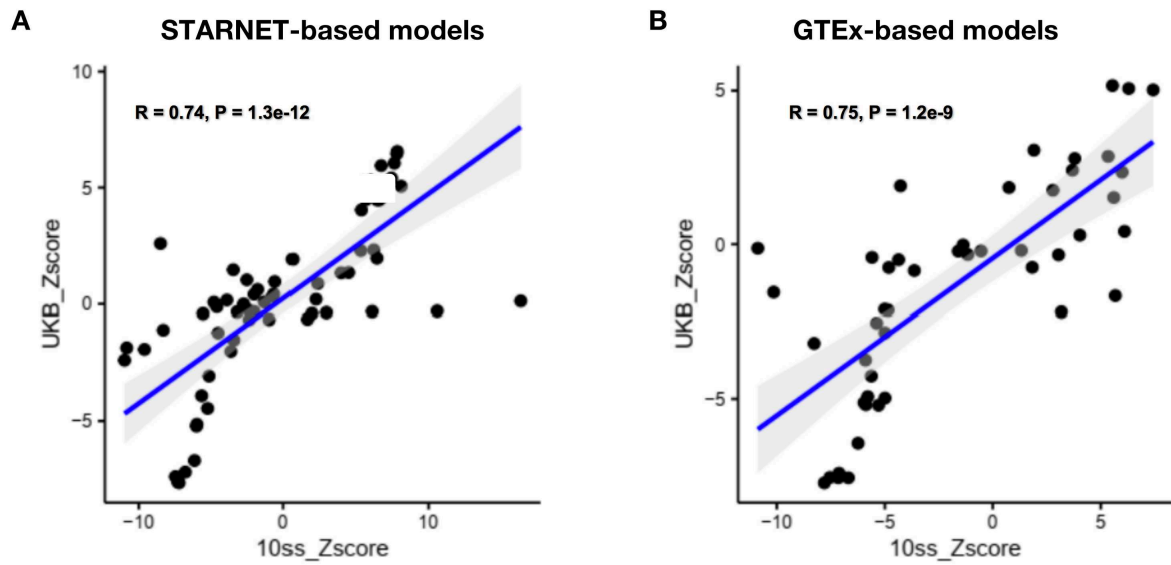
803 Supplementary Table 10. Association of TWAS genes' damaging mutation with quantitative
804 risk traits of CAD.

805 Supplementary Table 11. Lead variants resided in the regions of novel genes were associated
806 with lipid traits in human genotype data.

807 Supplementary Table 12. Expression-trait association statistics in mouse atherosclerosis
808 model from HMDP.

809 Supplementary Table 13. Oligo sequences for gene editing.

810 **Supplementary Figures**



811

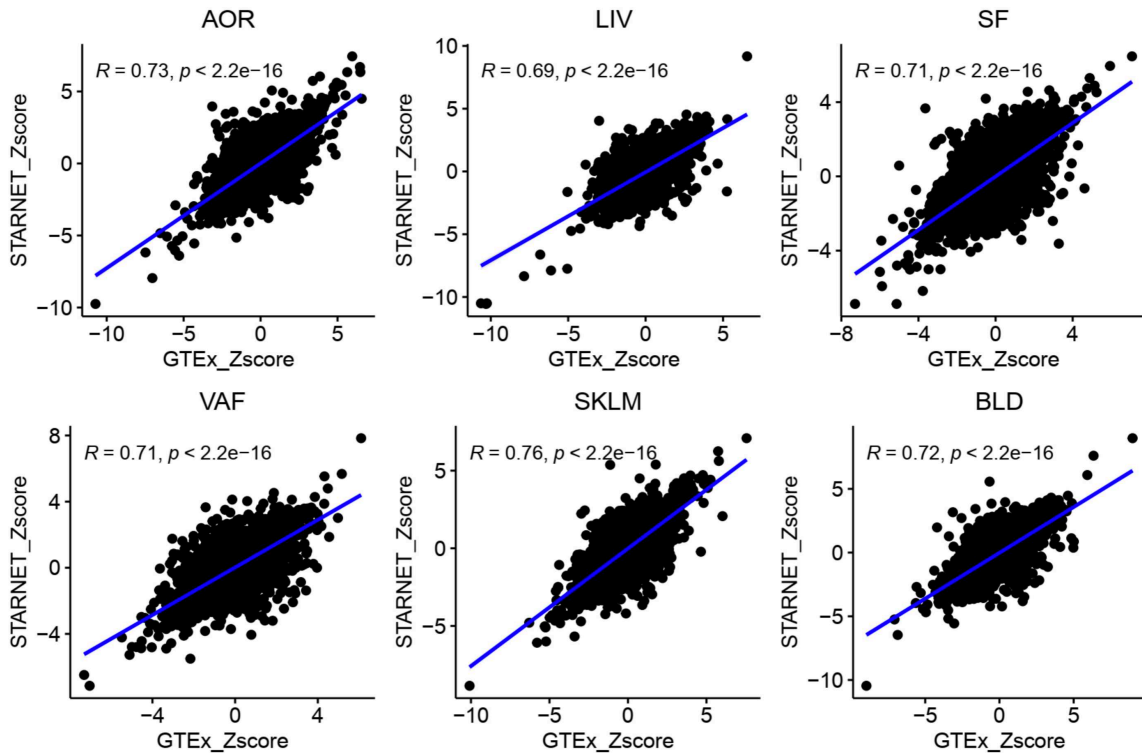
812 **Supplementary Fig. 1 Reproducibility of TWAS results within two reference models. A)**

813 Reproducibility of STARNET-based models. B) Reproducibility of GTEx-based models. Ten

814 CARDIoGRAMplusC4D cohorts (10ss) were used as the testing set, genotypes from UK

815 Biobank (UKB) were the validating set.

816

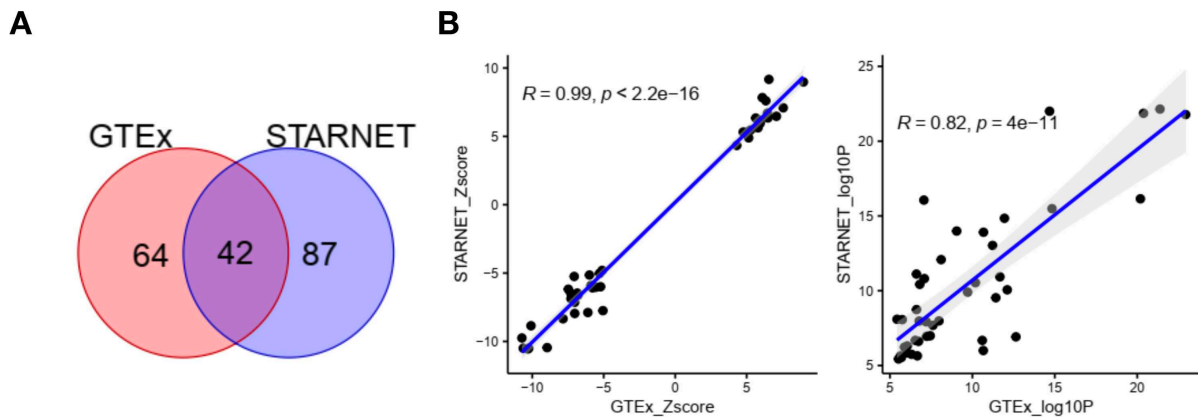


817

818 **Supplementary Fig. 2 Associations of predicted expressions with CAD are consistent**

819 **across tissues between STARNET- and GTEx-based models.**

820



821

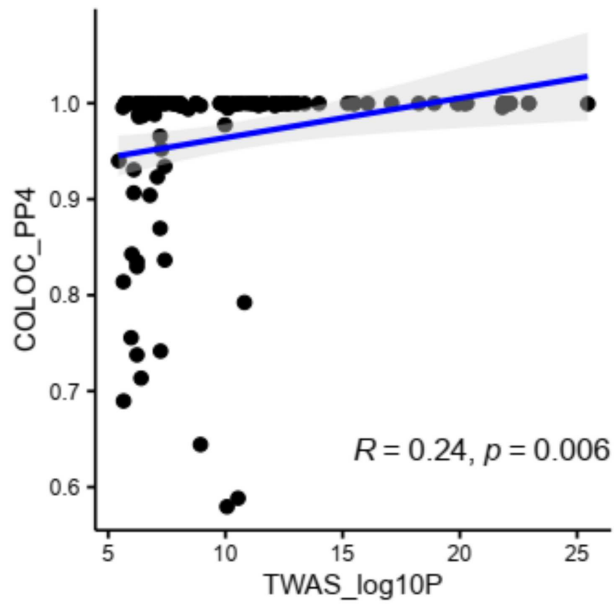
822 **Supplementary Fig. 3 Comparison of TWAS results between two reference models. A)**

823 **Venn diagram of transcriptome-wide significant gene-tissue pairs based on the two reference**

824 **models. There are 42 overlapping gene-tissue pairs (34 genes). B) The effect sizes (left) and**

825 **P values (right) of overlapping genes were consistent between the two reference-based**

826 **models.**



834

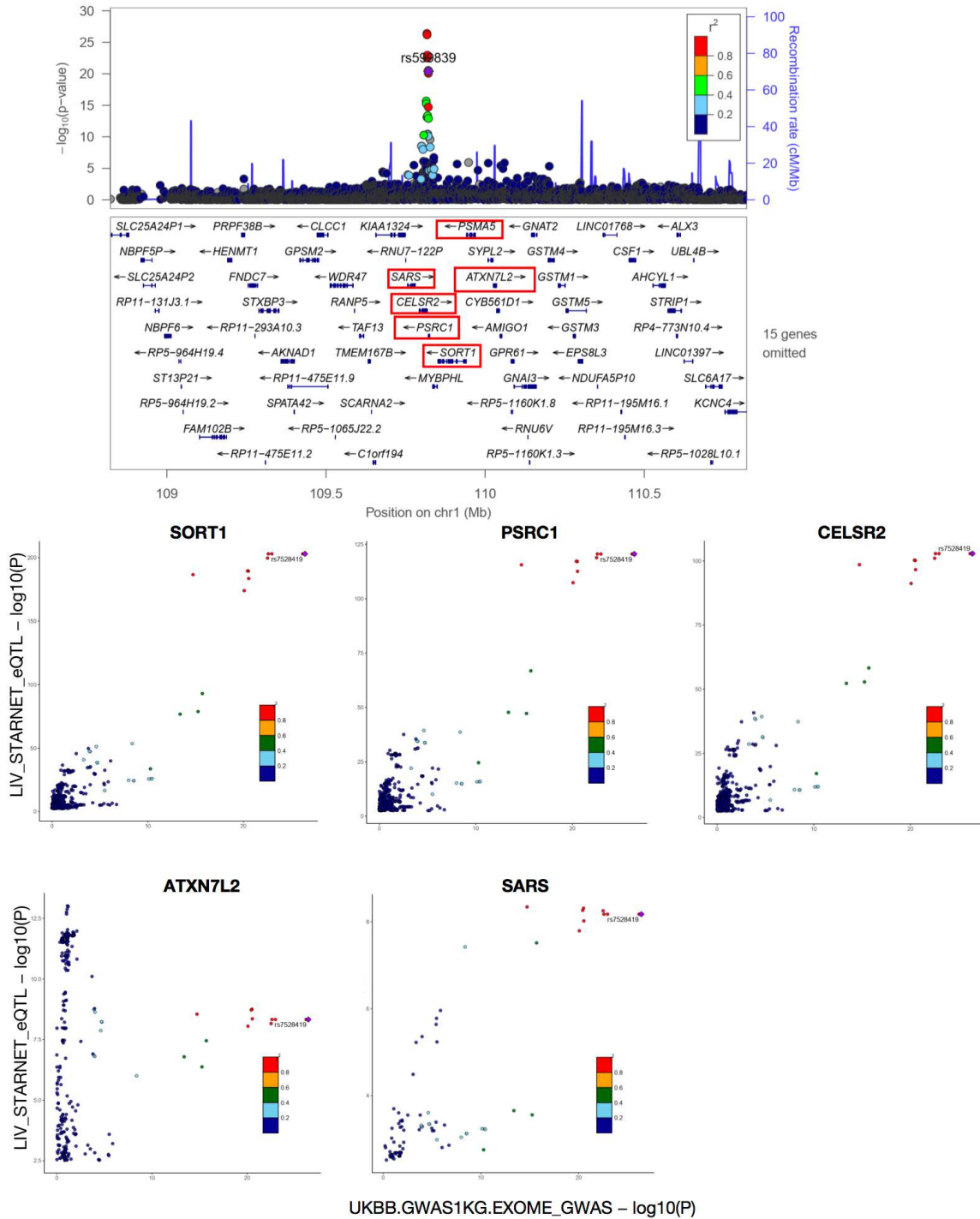
835 **Supplementary Fig. 5 Positive correlation between TWAS and colocalization statistics.**

836 The log10P statistics of TWAS genes were positively correlated with PP4 (the posterior

837 probabilities) statistics of colocalization analysis. Most TWAS genes have shared casual

838 variants between GWAS and eQTL signals as their PP4 approaches 1.

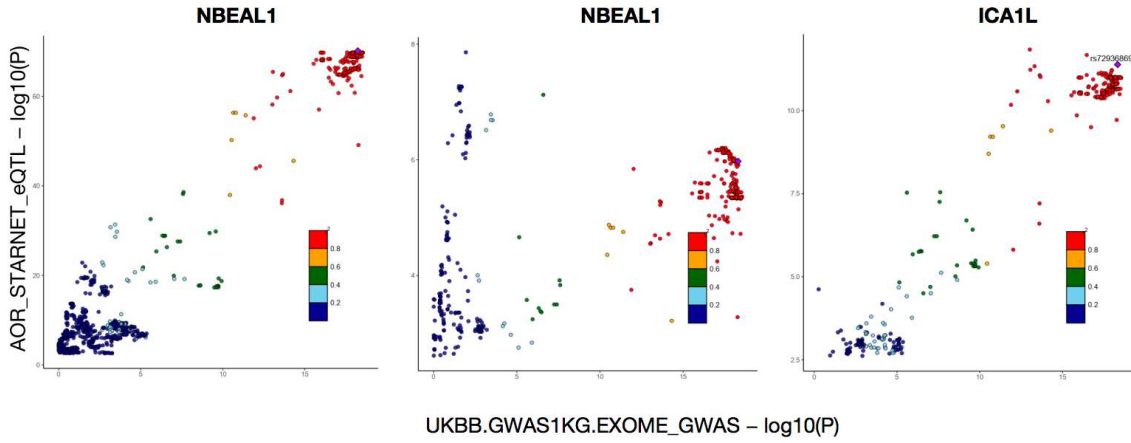
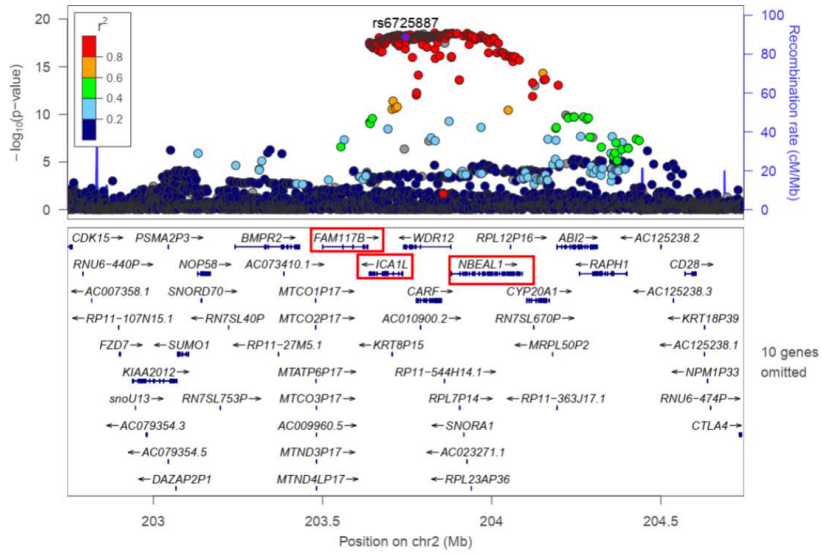
839



840

841 **Supplementary Fig. 6 Colocalization signals in liver tissue at 1p13.3.**

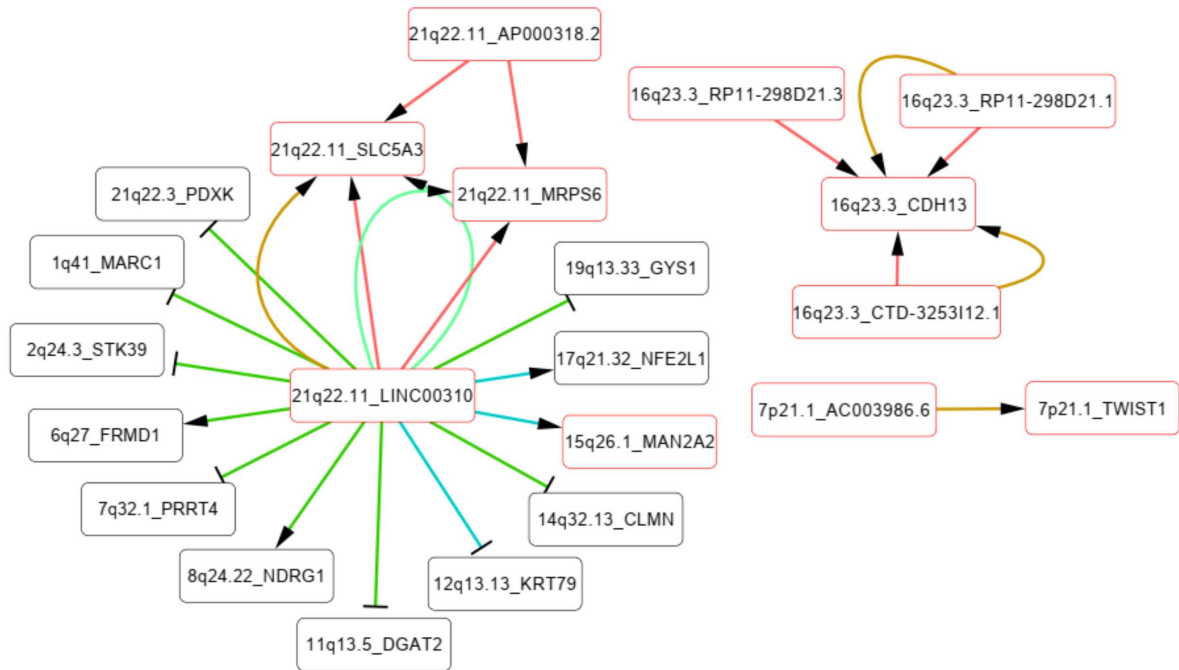
842



843

844 **Supplementary Fig. 7 Colocalization signals in aorta tissue at 2p33.2.**

845



846

847 **Supplementary Fig. 8 Co-expression network related to lncRNA genes.** Coding genes

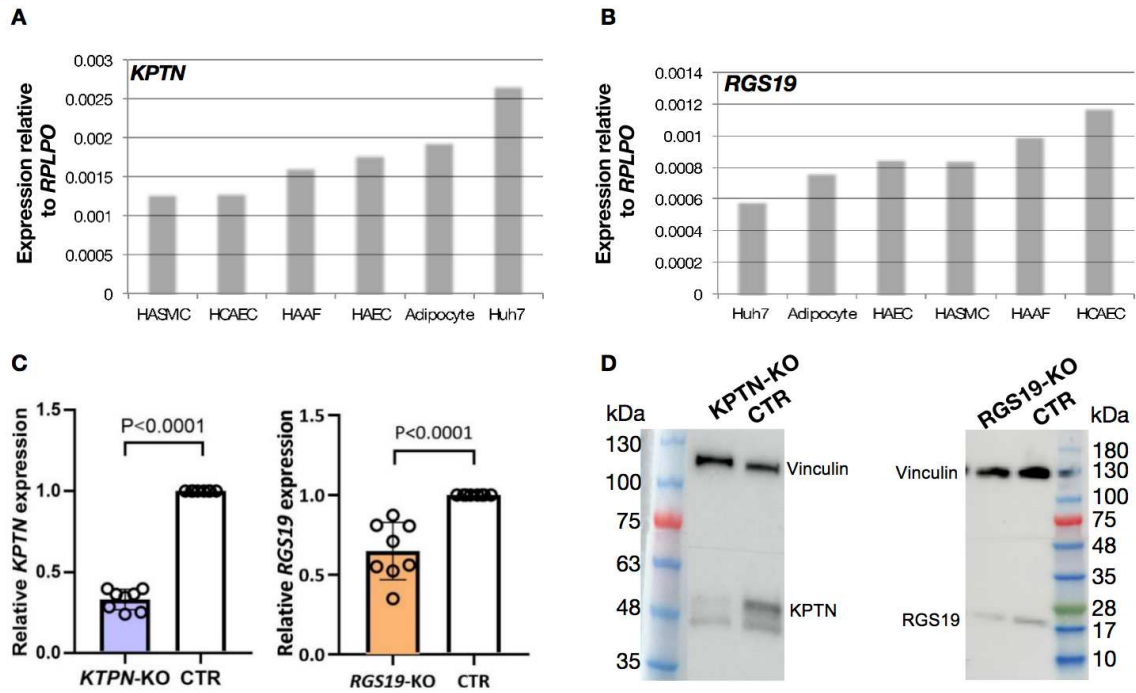
848 with co-expression relationship with TWAS lncRNA genes are linked by arrow or T-line.

849 Arrow suggests positive co-expression, and T-line suggests negative. TWAS genes are

850 indicated in red frame. Tissues of gene co-expression are showed in difference edge colors as

851 indicated.

852



853

854 **Supplementary Fig. 9** *KPTN* (A) and *RGS19* (B) expressions in multiple primary cells and
 855 cell lines. HASMC, human aorta smooth muscle cell; HCAEC, human coronary artery
 856 endothelium cell; HAAF, human aorta artery fibroblast; HAEC, human aorta endothelium
 857 cell and huh7, a human hepatoma cell line. (C) RNA levels of *KPTN* and *RGS19* were
 858 dramatically reduced in corresponding knockout lines (KO) in comparison to the control cell
 859 line (CTR), n=7. (D) The Western Blot image displays *KPTN* and *RGS19* reduction at protein
 860 level. Vinculin, 116kDa; *KPTN*, 48kDa; *RGS19*, 25kDa.

Supplementary Files

This is a list of supplementary files associated with this preprint. Click to download.

- [STable0702.xlsx](#)